Political Risk Modelling and Measurement From Stochastic Volatility Models

Sovan Mitra *

Abstract

The past decades have seen an unprecedented global rise in unforeseen political events, which have led to social unrest, economic declines and a renewed interest in political risk modelling. Whilst continuous time financial models have been developed for a range of risk factors, there is currently no method for political risk modelling. In this paper we propose a new model for political risk modelling; to the best of our knowledge this is the first model for continuous time stochastic volatility models. We derive a method for obtaining political risk states from a continuous time stochastic volatility model, and our model enables us to derive the evolution of political risk states over time. We derive two important properties of our political risk model: we find a solution for the characteristic function and prove weak convergence. Next, we derive a method for calculating standard risk measures for our political risk, namely Value at Risk, variance, moments, as well as upside and downside risk measurement. We also provide numerical experiments to illustrate our results.

Keywords: stochastic volatility; political risk; social risk; risk measurement; sustainability.

AMS subject classifications: 91G80, 93E11, 93E20

Acknowledgement: The author would like to thank Dr. Kirkby (School of Industrial and Systems Engineering, Georgia Institute of Technology, USA) and Dr. Nguyen (Department of Mathematics, Marist College, USA) for assistance in this paper.

*Department of Mathematics, University of Liverpool, Brownlow Hill, Liverpool, L69 3BX, UK Email: sovan.mitra@liverpool.ac.uk

1 Introduction

In the past decade political risk has gained significant attention (see for instance (Bekaert et al., 2016), (Chen et al., 2016) and (Dimic et al., 2015) to name a few); numerous political events have caused substantial political, social and economic consequences on societies. In Europe and in many parts of the West there have been a number of unexpected and widespread political outcomes, which have caused global concerns (see for instance (Beazer and Blake, 2018) and (Filippou et al., 2018)). Additionally, unlike other risk factors political risk causes direct impact on many social problems, such as civil disorder, public protests and crime. Consequently, political risk modelling has social importance as well as economic significance.

Whilst many risk factors have gained significant attention in mathematical finance (such as exchange rate risk, inflation risk, interest rate risk to name a few), the research on political risk modelling in the mathematical finance literature has been relatively sparse. The majority of studies in political risk have been undertaken by the empirical finance literature, using financial and economic variables as the basis for observing the impact of political risk. In the empirical finance literature, political risk has been studied to a greater extent (see for example (Pantzalis et al., 2000), (Clark, 2017) and (Snowberg et al., 2007)) and has been measured by asset volatility (see for instance (Bittlingmayer, 1998) and (Kelly et al., 2016)). There has been significant empirical analysis relating asset volatility and political risk, for example, stock market volatilities during the Great Depression (Bittlingmayer, 1998) are linked to political movements, and not just macroeconomic or financial variables. The rationale behind volatility as a political risk model is that political risk results in greater fluctuations in asset prices, causing increased volatility.

Whilst asset volatility has been used as a model of political risk, there exists no method for deriving the political risk model from mathematical finance models. Additionally, the empirical finance literature does not offer a theoretical framework for analysing or modelling political risk, rather they rely on response variables from empirical data and regression analyses. In this paper we propose a method for deriving the political risk model from typical stochastic volatility, continuous time finance models. We begin with a standard stochastic volatility model of asset prices (see (Cui et al., 2017b; Kirkby et al., 2017)), which is sufficiently comprehensive to capture a wide range of stochastic volatility dynamics. We then derive the political risk states from the stochastic volatility model, and the evolution of political risk states over time. We derive two important properties of our political risk model: firstly, the characteristic function, which enables us to fully describe the probability function of our model. Secondly, using a result from (Mijatovic and Pistorius, 2011), we prove our political risk model weakly converges to the original stochastic volatility model. This implies our political risk model provides a

credible model of political risk events and its evolution with respect to time. We then derive a method for calculating risk measures that can be applied to political risk. We derive equations for measuring political risk using coherent risk measures (Artzner et al., 2003) such as variance, downside risk, upside risk, as well as other popular risk measures such as Value at Risk and moments. To demonstrate our results, we conduct numerical experiments and provide results on political risk measurement.

This paper makes a number of contributions. Firstly, we devise (to the best of our knowledge) the first political risk model that is directly based on a continuous time finance, stochastic volatility model. Whilst other empirical literature has modelled the political risk, it does not use continuous time or stochastic volatility modelling, and the risk is not mathematically derived from the models. Secondly, we provide a method for modelling the evolution of political risk states over time, so that the political risk can be forecasted over time. Third, we derive the characteristic function of our political risk model, which enables us to fully describe its probability function and model other useful properties (such as risk). Fourthly, we show that our model weakly converges to the original stochastic volatility model and so our political risk model is a credible model for political risk events. Fifth, we derive a number of coherent and popular risk measures on political risk, which will allow individuals to measure the political risk in a quantitative approach. Finally, we provide numerical experiments to demonstrate our results.

The paper is organised as follows: in the next section we introduce the preliminaries and a literature review of relevant models. In the next section we introduce our political risk model, which can be applied to a wide range of generic stochastic volatility models. We describe the evolution of the political risk, to allow us to model political risk over time. In the next section we derive the characteristic function for an asset that follows our political risk model, and show that it weakly converges to the original continuous time model. In the next section we derive our risk measures and then conduct numerical experiments to calculate political risk. We finally end with a conclusion.

2 Preliminaries

Let there exist a probability space $\{\Omega, \mathcal{F}, \mathbb{P}\}$ where Ω denotes the sample space, $\mathcal{F}$ denotes a collection of events in Ω with probability measure $\mathbb{P}$, and we have a filtered probability space $\{\Omega, \mathcal{F}, \{\mathcal{F}_t\}_{t\geq 0}, \mathbb{P}\}$. The set $\{\mathcal{F}_t\}$ denote the set of information that is available to the observer up to time t , so that

$$\mathcal{F}_{t_1} \subseteq \mathcal{F}_{t_2} \subseteq \mathcal{F}_{\tilde{T}} < \infty, \ \forall t_1 < t_2 < \tilde{T}.$$

The set $\{\mathcal{F}_t\}$, $t \in [0, \tilde{T}]$, is also known as a filtration. Furthermore, for a given stochastic process $X(t)$, as more information is revealed to an observer as time t progresses, we introduce the filtration $\mathcal{F}_t^X$ which denotes the information generated by process $X(t)$ on the interval $[0, t]$. Finally, assume we have the probability space $\{\Omega, \mathcal{F}, \mathbb{P}\}$ then we define a change of measure from $\mathbb{P} \sim \mathbb{Q}$ to be the probability space $\{\Omega, \mathcal{F}, \mathbb{Q}\}$.

By Girsanov's Theorem with respect to stochastic differential equations and change of probability measures, let us assume we have a family of information sets $\mathcal{F}_t$ over a period $[0, \tilde{T}]$. We define over $[0, \tilde{T}]$ the random process (also known as the Doleans exponential) $\varkappa_t$:

$$\varkappa_t = \exp\left\{-\int_0^t \hat{\gamma}(u) dB^{\mathbb{P}}(u) - \frac{1}{2}\int_0^t \hat{\gamma}^2(u) du\right\},$$

where $B^{\mathbb{P}}(t)$ is the Wiener process under probability measure $\mathbb{P}$ and $\hat{\gamma}(t)$ is an $\mathcal{F}_t$-measurable process that satisfies the Novikov condition

$$\mathbb{E}^{\mathbb{P}}\left[\exp\left\{\frac{1}{2}\int_0^t \hat{\gamma}^2(u) du\right\}\right] < \infty, t \in [0, \tilde{T}].$$

We then have $B^{\mathbb{Q}}(t)$ is a Wiener process with respect to $\mathcal{F}_t$ under probability measure $\mathbb{Q}$, where $B^{\mathbb{Q}}(t)$ is defined by

$$B^{\mathbb{Q}}(t) = B^{\mathbb{P}}(t) + \int_0^t \hat{\gamma}(u) du, t \in [0, \tilde{T}].$$

The Black and Scholes option pricing model (Black and Scholes, 1973) is the benchmark option pricing model that provides a closed form solution of European call options $C_{BS}(X(t))$:

$$C_{BS}(X(0), \hat{T}, r, \sigma, K) = X(0)\Psi(d_1) - Ke^{-r\hat{T}}\Psi(d_2),$$

where

$$d_1 = \frac{\log\left(X(0)/K\right) + \left(r + \sigma^2/2\right)\hat{T}}{\sigma\sqrt{\hat{T}}}, \qquad d_2 = d_1 - \sigma\sqrt{\hat{T}},$$

where $X(t)$ is the stock price that follows Geometric Brownian motion

$$dX(t)/X(t) = \mu dt + \sigma dB(t).$$

In the model $\mu \in \mathbb{R}$ denotes the drift and represents the typical long term growth of the firm, σ denotes volatility, $B(t)$ is a Wiener process, $\hat{T}$ is the expiration date, $\Psi(\cdot)$ is the standard normal cumulative distribution function, r is the riskfree rate of interest and K is the strike price. The price of a European call option is also determined by risk neutral valuation

$$C_{RN}(X(t), K, \hat{T}) = e^{-r(\hat{T}-t)}\mathbb{E}^{\mathbb{Q}}[X(\hat{T}) - K]^+.$$

Political risk can be defined as the risk associated with political events, such as political elections. Whilst political risk has been acknowledged as a significant impact on asset prices, it

has not been researched as extensively as other risk factors, for example inflation. The literature on political risk is practically non-existent in the mathematical finance literature, however it has been more extensively researched in the empirical finance literature. In the empirical finance literature political risk has been measured by multiple factors, such as abnormal stock market returns (see for instance (Pantzalis et al., 2000)), stock market indices (such as the S&P 500, NASDAQ and Dow Jones), interest rates and oil prices (see for instance (Snowberg et al., 2007)) . Such models are not applicable to continuous time mathematical finance models, they do not provide a theoretical model for political risk, and their risk modelling is confined to measuring risk only at specific political dates.

As mentioned before, political risk is measured by asset volatility (see for instance (Bittlingmayer, 1998) and (Kelly et al., 2016)), for example, stock market volatilities are linked to political movements (Bittlingmayer, 1998). This measure of political risk also has conceptual advantages because larger political risk should create greater fluctuations in asset prices, which would increase volatility. Moreover, the modelling of asset volatility has a well developed body of research, with many financial models already available. Hence the political risk modelling can be modeled to a greater degree of sophistication.

The initial models of volatility considered volatility as a constant (Black and Scholes, 1973), however empirical evidence (such as the leverage effect) has motivated new volatility models. The first development of volatility modelling was time dependent volatility modelling (see for example (Wilmott et al., 1998)):

$$dX(t)/X(t) = \mu dt + \sigma(t) dB(t).$$

In this model volatility $\sigma(t)$ is a deterministic function of time t, and so is no longer constant. The work of (Merton, 1973) derived the option pricing equation associated with this volatility model, using the standard Black-Scholes equation and volatility is replaced by σ_c, where

$$\sigma_c = \sqrt{\frac{1}{\hat{T}-t}\int_t^{\hat{T}} \sigma^2(\tau)d\tau},$$

so that d_1 and d_2 in the Black-Scholes equation become:

$$\begin{aligned} d_1 &= \frac{\log\left(\frac{X(t)}{K}\right) + \mu(\hat{T}-t) + \frac{1}{2}\int_t^{\hat{T}} \sigma^2(\tau)d\tau}{\sqrt{\int_t^{\hat{T}} \sigma^2(\tau)d\tau}}, \\ d_2 &= \frac{\log\left(\frac{X(t)}{K}\right) + \mu(\hat{T}-t) - \frac{1}{2}\int_t^{\hat{T}} \sigma^2(\tau)d\tau}{\sqrt{\int_t^{\hat{T}} \sigma^2(\tau)d\tau}}. \end{aligned}$$

Another development in volatility modelling has been local volatility modelling. In local volatility the volatility is a function of stock price and time, that is $\sigma = f(X(t), t)$. The local

volatility models retain market completeness in option pricing, hence unique option prices can be calculated. Examples of local volatility models include the Constant Elasticity of Variance model (CEV), which is given by (Cox and Ross, 1976)

$$\begin{aligned} \frac{dX(t)}{X(t)} &= \mu dt + \sigma(X(t))dB(t), \\ \sigma(X(t)) &= \tilde{\kappa}X^{\tilde{\eta}-1}(t), \ for \ \{\tilde{\eta} \in \mathbb{R} | 0 \leq \tilde{\eta} \leq 1\}, \tilde{\kappa} \in \mathbb{R}^{+}. \end{aligned}$$

For $\tilde{\kappa} = 0$ we obtain Bachelier's model of stock prices, while $\tilde{\kappa} = 1$ gives the Geometric Brownian Motion model. The CEV model has been developed over the years (for instance (Cox and Ross, 1976), (Cox et al., 1985) and (Schroder, 1989)), and by appropriate choices of $\tilde{\eta}$ and $\tilde{\kappa}$ one can fit CEV to volatility smiles, see (Beckers, 1980).

Dupire's local volatility model (Dupire, 1994) enables one to derive Dupire's equation by application of the Fokker-Planck equation:

$$\frac{\partial C(t)}{\partial \hat{T}} = \sigma^2(X(t), \hat{T}).\frac{X^2(t)}{2}.\frac{\partial^2 C(t)}{\partial X^2(t)} - (r-\delta)X(t).\frac{\partial C(t)}{\partial X(t)} - \delta.C(t), \tag{1}$$

where δ is the asset dividend. One can derive from equation (1) that:

$$\sigma(X(t), \hat{T}) = \sqrt{\frac{\frac{\partial C(t)}{\partial \hat{T}} + (r-\delta)X(t)\frac{\partial C(t)}{\partial X} + \delta.C(t)}{\frac{X^2(t)}{2}\frac{\partial^2 C(t)}{\partial X^2(t)}}}. \tag{2}$$

The equation (2) therefore implies that local volatility $\sigma(X(t), \hat{T})$ can be fully described by option data, however, it can be noticed that calculating $\sigma(\cdot)$ requires partial differentials with respect to $\hat{T}$ and K. Consequently, we require a continuous set of options data in K and $\hat{T}$, and this is highly unrealistic as quoted option prices tend to suffer from significant illiquidity (Nordén, 2003).

The most comprehensive development in volatility modelling has been stochastic volatility, which is a development beyond local volatility models. The stochastic volatility model can take into account more empirical properties that are not present in local volatility models (Musiela and Rutkowski, 2005), such as the clustering effect, fatter tail distributions, implied volatility smiles and time scaling effects. Stochastic volatility models differ from other volatility models in that volatility is driven by another Wiener process. The generic stochastic volatility model is given by

$$\begin{aligned} dX(t)/X(t) &= \mu_1(X(t), t)dt + \sigma(t)dB^1(t), \\ \sigma(t) &= f(dB^2(t)), \end{aligned}$$

where volatility is a function of a stochastic process that is driven by another (but possibly correlated) Wiener process $dB^2(t)$, so that

$$corr(dB^1(t), dB^2(t)) = \rho dt, \ where \ \{\rho \in \mathbb{R} | -1 \leq \rho \leq 1\}.$$

The probability space $(\Omega, \mathcal{F}, \mathbb{P})$ is $\Omega = \mathcal{C}([0,\infty) : \mathbb{R}^2)$, with filtration $\{\mathcal{F}_t\}_{t\geq 0}$ to represent information on two Wiener processes $\{B^1(t), B^2(t)\}$.

One of the first stochastic volatility models is (Johnson and Shanno, 1987), where

$$d\sigma(t) \;=\; \mu_2\sigma(t)dt + \sigma^{\tilde{\kappa}}(t)\tilde{\eta}dB^2(t),\ for\ \{\tilde{\kappa},\tilde{\eta}\in\mathbb{R}|\tilde{\kappa},\tilde{\eta}\geq 0\}.$$

The option prices in (Johnson and Shanno, 1987) are obtained by Monte Carlo methods due to analytical intractability. An alternative stochastic volatility is given in (Scott, 1987) where volatility follows an Ornstein-Uhlenbeck process:

$$d\sigma(t) \;=\; \mu_2(\tilde{\kappa}-\sigma(t))dt + \tilde{\eta}dB^2(t),\ for\ \{\tilde{\kappa},\tilde{\eta}\in\mathbb{R}|\tilde{\kappa},\tilde{\eta}\geq 0\}.$$

One of the more popular stochastic volatility models is the Hull-White Model (Hull and White, 1987):

$$d\sigma^2(t)/\sigma^2(t) = \mu_2 dt + \tilde{\eta}dB^2(t),\ for\ \{\tilde{\kappa},\tilde{\eta}\in\mathbb{R}|\tilde{\kappa},\tilde{\eta}\geq 0\},$$

where

$$\hat{\sigma}^2 = \frac{1}{\tilde{T}-t}\int_t^{\tilde{T}}\sigma^2(s)ds,$$

enables one to obtain option prices using the Black-Scholes option pricing equation, with volatility $\hat{\sigma}^2$.

The Heston stochastic volatility model (Heston, 1993) stands out from other stochastic volatility models as it provides an analytic solution for European options, and the volatility model takes in account correlation between Wiener processes $corr(dB^1(t), dB^2(t)) = \rho dt$. The Heston model volatility process is give by

$$d\sigma^2(t) \;=\; \mu_2(\tilde{\kappa}-\sigma^2(t))dt + \tilde{\eta}\sigma(t)dB^2(t),\ for\ \{\tilde{\kappa},\tilde{\eta}\in\mathbb{R}|\tilde{\kappa},\tilde{\eta}\geq 0\}.$$

The model for $d\sigma^2(t)$ originated from (Cox et al., 1985) and an analytical solution for options is found using Fourier transforms. As one can see, whilst the modelling of volatility has been substantial in mathematical finance, there has been little development in political risk modelling.

3 Political Risk Model

In this section we derive our political risk model from a continuous time, stochastic volatility model. Let us assume that our asset model is defined by

$$dX(t)/X(t) \;=\; \alpha dt + \zeta(\sigma(t))dB^1(t) + (e^{\lambda(t)}-1)d\kappa(t), \tag{3}$$

with stochastic volatility process

$$d\sigma(t) \;\; = \;\; v(\sigma(t))dt + \beta(\sigma(t))dB^2(t), \tag{4}$$

where $v(\sigma(t))$ is the drift process for $\sigma(t)$, $\beta(\sigma(t))$ is the coefficient of the Brownian motion $dB^2(t)$, $corr(dB^1(t)dB^2(t)) = \rho dt$, such that $\{\rho \in \mathbb{R}| -1 \leq \rho \leq 1\}$. The Poisson process is $\kappa(t)$ with a jump rate γ , and $\lambda(t) \sim \lambda$ is the jump amplitude; both are independent of $dB^1(t), dB^2(t)$. The risk neutral drift α is given by

$$\alpha = r - u - \gamma\iota,$$

where $r \in \mathbb{R}^+$ is the riskless rate, $\iota = \mathbb{E}[e^\lambda - 1]$, $u \in \mathbb{R}^+$ is the continuous dividend yield. By application of Ito's lemma we can re-express our stock price model as

$$d(log(X(t)) = \left(\alpha - \frac{1}{2}\zeta^2(\sigma(t))\right)dt + \zeta(\sigma(t))dB^1(t) + d\left[\sum_{k=1}^{k=\kappa(t)} Z_k(t)\right]. \tag{5}$$

We now define our political risk model. A political risk model allocates different latent political states according to the level of political risk (Bodie et al., 2019). Consequently, political risk is modeled in a similar way to credit risk, where credit ratings (such as AAA, BBB etc.) denote different levels of credit risk. Credit risk can be modelled using continuous time Markov chains (Lu, 2009) and similarly political risk is modelled as a finite state, continuous time, Markov chain stochastic process, on the risk neutral probability space $\{\Omega, \mathcal{F}, \mathbb{Q}\}$. There exists a finite set of (Markov) states $\mathcal{S}$, where

$$\mathcal{S} := \{1, 2, ..., n\}, \textit{such that } \{n \in \mathbb{N}^+ | n < \infty\}.$$

The number n models the number of political states that can occur. Each Markov state represents a different political state, and is associated with a different level of volatility $\boldsymbol{\sigma}$, that is $\boldsymbol{\sigma} := \{\sigma_1, \sigma_2, ..., \sigma_n\}$, such that $\sigma_{j-1} < \sigma_j, \forall j \in \{1, 2, ..., n\}$. If we denote the state at time t by $\theta(t)$ then our political risk model has state transition probabilities

$$\mathbb{Q}(\theta(t + \Delta t) = j | \theta(t) = k) = \mathbb{Q}(\theta(t + \Delta t) = j | \theta(t) = k, \theta(\tau)), \forall k, j \in \mathcal{S}, 0 \leq \tau \leq t,$$

that is state transition probabilities are not dependent on state histories for $\theta(\tau)$, $\forall \tau$, such that $0 \leq \tau \leq t$. This is a non-restrictive assumption given that many social phenomena are modelled by Markov chains, where past states do not affect state transition probabilities. The continuous time Markov chain $\theta(t)$ is characterized by the transition rate matrix $\mathbf{P} = [p_{jk}]_{(j,k)\in\mathcal{S}\times\mathcal{S}}$ that satisfies the following conditions:

$$\begin{cases} p_{jj} \leq 0, & \forall j \in \mathcal{S}, \\ p_{jk} \geq 0, & \forall k \neq j \in \mathcal{S}, \\ \sum_{k\in\mathcal{S}} p_{jk} = 0, & \forall j \in \mathcal{S}. \end{cases} \tag{6}$$

We now wish to perform the mapping σ from equation (4) to $\boldsymbol{\sigma}$, where $\boldsymbol{\sigma} :\rightarrow \{\sigma_1, \sigma_2, ..., \sigma_n\}$, to derive the political states from our model of the underlying asset. The number n represents the number of distinct political states that can occur. Additionally, there is the obvious difficulty in defining and characterizing the political states, which presents many challenges from a modelling perspective. Our approach to this problem is to parametrize these states in terms of a defined CTMC representation of a latent volatility process. As the latent volatility process evolves, the associated political state transitions accordingly. That is, to each level of latent volatility $\boldsymbol{\sigma} := \{\sigma_1, \sigma_2, ..., \sigma_n\}$, we associate a distinct political state, such that $\sigma_{j-1} < \sigma_j, \forall j \in \{1, 2, ..., n\}$.

Let $\overline{\eta}(t) := \mathbb{E}[\sigma(t)|\sigma(0)]$, $\overline{\nu}(t) = \sqrt{Var(\sigma(t)|\sigma(0))}$, where $Var(.)$ denotes variance, and $\tau = T/2$. The constant T is defined as follows: let us consider the asset price $X(t)$ trading on the finite trading horizon $t \in [0, T]$ and $t \in \mathbb{R}^+$. We define M monitoring dates at which times the process $X(t)$ is observed, such that $0 = t_0 < t_1 < t_2.... < t_M = T$. Moreover, the associated *realized variance* Λ_M is given by

$$\Lambda_M = \frac{L}{M} \sum_{m=1}^{M} \left(\log \frac{X(t_m)}{X(t_{m-1})} \right)^2,$$

where $L = \dfrac{M}{T}$ (if T is measured in years), and L is a normalization constant. Hence weekly monitoring over T=1 year gives $L = 52$ and $M = 52$. In particular, the realized variance allows us to infer knowledge of the underlying latent state by measuring the realized squared-returns of the observable asset process. It is through this process that we will calculate measures of political risk.

Let $\tau = T/2$, as previously discussed, many volatility models $\sigma(t)$ follow a stochastic differential equation or a Brownian motion process. Consequently, $\sigma(\tau)$ approximates a Gaussian distribution, and this is consistent with empirical data. Therefore we apply the mapping $\{\sigma_1, \sigma_2, ..., \sigma_n\}$ as follows

$$\sigma_k = \sigma(0) + \nu \sinh \left(\hat{\nu}_2 \left(\frac{k}{n} \right) + \hat{\nu}_1 \left(1 - \frac{k}{n} \right) \right), k \in \{2, ..., n-1\}, \tag{7}$$

where

$$\begin{aligned} \nu &> |\sigma_n - \sigma_1|, \\ \hat{\nu}_1 &= \sinh^{-1} \left(\frac{\sigma_1 - \sigma(0)}{\nu} \right), \hat{\nu}_2 = \sinh^{-1} \left(\frac{\sigma_n - \sigma(0)}{\nu} \right), \\ \sigma_n &= \overline{\eta}(\tau) + \hat{c}\overline{\nu}(\tau), \end{aligned}$$

where $\hat{c} \in \mathbb{R}^+$ is a specified constant. To determine σ_1 we must distinguish between two classes of stochastic volatility processes. We have

$$\begin{aligned} \sigma_1 &= \max(\overline{\alpha}, \overline{\eta}(\tau) - \hat{c}\overline{\nu}(\tau)), \text{ if the state-space of } \sigma(t) \quad \text{is} \quad [0, \infty), \\ \sigma_1 &= \overline{\eta}(\tau) - \hat{c}\overline{\nu}(\tau), \text{ if the state-space of } \sigma(t) \quad \text{is} \quad (-\infty, \infty), \end{aligned}$$

where $\overline{\alpha} \in \mathbb{R}^+$ is a specified constant. We note that the constants $\overline{\alpha}, \hat{c}$ will vary for each stochastic volatility model (e.g Heston model, Stein-Stein model, etc.).

We require that our political risk model satisfies local consistency conditions and weak convergence to $\sigma(t)$. We therefore impose the condition that the first two moments of $\sigma(t)$ are consistent with our model, that is

$$\begin{aligned}\mathbb{E}[\sigma(t+\Delta t) - \sigma(t)] &= v(\sigma_k)\Delta t, \\ \mathbb{E}[\sigma(t+\Delta t) - \sigma(t)]^2 &= \beta^2(\sigma_k)\Delta t.\end{aligned}$$

We also require $\mathbf{z} = \{z_1, z_2, ..., z_{n-1}\}$, where $z_k = \sigma_k - \sigma_{k-1}$, such that

$$0 < \max_{1 \le k \le n-1} z_k \le \min_{1 \le k \le n} \frac{\beta^2(\sigma_k)}{|v(\sigma_k)|}.$$

This condition implies that

$$\beta^2(\sigma_k) \ge z_{k-1}v^-(\sigma_k) + z_k v^+(\sigma_k), \tag{8}$$

where $x^\pm = \max(0, \pm x)$. With (Lo and Skindilias, 2014) we obtain the transition rate matrix $\mathbf{P}$ and therefore fully specify the political risk model:

$$p_{jk} = \begin{cases} \dfrac{v^-(\sigma_k)}{z_{k-1}} + \dfrac{\beta^2(\sigma_k) - (z_{k-1}v^-(\sigma_k) + z_k v^+(\sigma_k))}{z_{k-1}(z_{k-1}+z_k)}, & \textit{for } k = j-1, \\ \dfrac{v^+(\sigma_k)}{z_{k-1}} + \dfrac{\beta^2(\sigma_k) - (z_{k-1}v^-(\sigma_k) + z_k v^+(\sigma_k))}{z_k(z_{k-1}+z_k)}, & \textit{for } k = j+1 \\ -p_{j,j-1} - p_{j,j+1}, & \textit{for } k = j \\ 0 & \textit{for } |k-j| > 1. \end{cases} \tag{9}$$

We note that equation (8) will guarantee that $p_{ij} \ge 0$ for $i \ne j$. Additionally, from equation (9), it can be proven that p_{ij} satisfies all the conditions specified in (6).

We have now derived our political risk model from the continuous time asset pricing model, with stochastic volatility dynamics. Hence our model can take into account a range of volatility modelling dynamics, and one can derive the political risk model. The elements p_{jk} in $\mathbf{P}$ tell us the rate at which there is movement between each political state, hence we can fully describe the changes between political states. As discussed in Section 4, this model will approach the original parameterizing stochastic volatility process as the state-space is refined. However, for any number of political states n, the parametrization results in a valid probability model, governed by $\mathbf{P}$.

4 Characteristic Function and Weak Convergence Properties

We now wish to prove in this section that our political risk model is weakly convergent to the original stochastic volatility model and the characteristic function of our model. The weak

convergence proof is an important property because it demonstrates that our model is a viable representation of the original stochastic volatility model. It demonstrates that as we increase the number of political states, our model will approach a well-behaved (and easily interpretable) stochastic volatility process.

Theorem 1. *The asset pricing model*

$$dX(t)/X(t) = \alpha dt + \zeta(\sigma(t))dB^1(t) + (e^{\lambda(t)} - 1)d\kappa(t),$$

with stochastic volatility

$$d\sigma(t) \;=\; v(\sigma(t))dt + \beta(\sigma(t))dB^2(t),$$

is equivalent to

$$dS(t) = \left(\alpha - \frac{\zeta^2(\sigma(t))}{2} - \rho g(\sigma(t))\right)dt + \sqrt{(1-\rho^2)}\zeta(\sigma)dB^*(t) + d\left[\sum_{k=1}^{\kappa(t)} Z_k(t)\right],$$

with

$$d\sigma(t) = v(\sigma(t))dt + \beta(\sigma(t))dB^2(t),$$

where

$$\begin{aligned}
B^*(t) &:= \frac{B^1(t) - \rho B^2(t)}{\sqrt{(1-\rho^2)}}, \\
S(t) &= \log\left(\frac{X(t)}{X(0)}\right) - \tilde{h}(\sigma(t), \sigma(0)), \\
\tilde{h}(\sigma(t), \sigma(0)) &= \rho(h(\sigma(t)) - h(\sigma(0))), \\
h(x) &= \int_c^x \frac{\zeta(z)}{\beta(z)}dz, \\
g(x) &:= \mathcal{L}(h(x)) = v(\sigma(x))h'(x) + \frac{1}{2}\beta^2(x)h''(x).
\end{aligned}$$

The Markov chain (alternatively called the regime switching) approximation of $dS(t)$ is given by $d\tilde{S}(t)$, where

$$d\tilde{S}(t) = \tilde{\alpha}(\theta(t))dt + \tilde{\sigma}(\theta(t))dB^*(t) + d\left[\sum_{k=1}^{\kappa(t)} Z_k(t)\right], \forall \theta(t) \in \mathcal{S},$$

with

$$\begin{aligned}
\tilde{\alpha}(\theta(t)) &= \alpha - \left(\frac{\zeta^2(\sigma_{\theta(t)})}{2}\right) - \rho g(\sigma_{\theta(t)}), \\
\tilde{\sigma}(\theta(t)) &= \sqrt{(1-\rho^2)}\zeta(\sigma_{\theta(t)}).
\end{aligned}$$

Proof. Let

$$B^*(t) \;:=\; \frac{B^1(t) - \rho B^2(t)}{\sqrt{(1-\rho^2)}},$$

then $\mathbb{E}[dB^*(t)dB^2(t)] = 0$. Hence $B^*(t), B^2(t)$ are two independent Brownian motions. From the above equation, we have

$$dB^1(t) \;=\; \rho dB^2(t) + \sqrt{(1-\rho^2)}dB^*(t),$$

we substitute this into equation (5) and this yields

$$\begin{aligned} d(\log(X(t))) &= \left(\alpha - \frac{1}{2}\zeta^2(\sigma(t))\right)dt + \zeta(\sigma(t))(\rho dB^2(t) + \sqrt{(1-\rho^2)}dB^*(t)) \\ &+ d\left[\sum_{k=1}^{\kappa(t)} Z_k(t)\right]. \end{aligned} \tag{10}$$

Let $h(x)$, $\tilde{h}(.,.), g(x)$ be defined as above. If we apply Ito's Lemma we have

$$d\tilde{h}(\sigma(t), \sigma(0)) = \rho dh(\sigma(t)) = \rho g(\sigma(t))dt + \rho v(\sigma(t))dB^2(t),$$

and so equation (10) becomes

$$d(\log(X(t)) = \left(\alpha - \frac{1}{2}\zeta^2(\sigma(t))\right)dt + d\tilde{h}(\sigma(t), \sigma(0)) - \rho g(\sigma(t))dt + d\left[\sum_{i=1}^{\kappa(t)} Z(t)\right].$$

Now, define

$$S(t) := \log\left(\frac{X(t)}{X(0)}\right) - \tilde{h}(\sigma(t), \sigma(0)).$$

then we can write

$$\begin{aligned} dS(t) &= \left(\alpha - \frac{\zeta^2(\sigma(t))}{2} - \rho g(\sigma(t))\right)dt + \sqrt{(1-\rho^2)}dB^*(t) + d\left[\sum_{i=1}^{\kappa(t)} Z(t)\right], \\ d\sigma(t) &= v(\sigma(t))dt + \beta(\sigma(t))dB^2(t). \end{aligned}$$

We recall that in our political risk model we have $\sigma(t) :\to \boldsymbol{\sigma}$, that is the stochastic process is governed by Markov chains, or also known as a regime switching model. We also note that $S(t)$ and $\sigma(t)$ are now driven by independent Brownian motions in the previous equations, given that we have specified $dB^*(t)$ and $dB^2(t)$ as independent. We can therefore model $dS(t)$ by an equivalent regime switching model $d\tilde{S}(t)$, that is

$$d\tilde{S} = \tilde{\alpha}(\theta(t))dt + \tilde{\sigma}(\theta(t))dB^*(t) + d\left[\sum_{i=1}^{\kappa(t)} Z(t)\right], \forall \theta(t) \in \mathcal{S},$$

where

$$\begin{aligned}\tilde{\alpha}(\theta(t)) &= \alpha - \frac{\zeta^2(\tilde{\sigma}(\theta(t)))}{2} - \rho g(\sigma_{\theta(t)}),\\ \tilde{\sigma}(\theta(t)) &= \sqrt{(1-\rho^2)}\zeta(\sigma_{\theta(t)}).\end{aligned}$$

□

We now wish to prove the weak convergence results, that is that our political risk model converges to the original stochastic model.

Theorem 2. *For a political risk model where* $\boldsymbol{P}$ *follows equation* (9) *then* $(\sigma_{\theta(t)}, \tilde{S}(t))$ *converges weakly (in distribution) to the original model* $(\sigma(t), S(t))$.

Proof. First let us define the diffusion process $\overline{S}(t)$ such that it follows $S(t)$ and excludes the jump process; similarly let us define $\overline{S}^n(t)$ as the diffusion process that follows $\tilde{S}(t)$, with n political states, and excludes the jump process. We now prove that $(\sigma_{\theta(t)}, \overline{S}^n(t))$ converges weakly to $(\sigma_{\theta(t)}, \overline{S}(t))$. Let us fix $\sigma(t) = \sigma$ and $\overline{S}(t) = s$. We recall $B^*(t)$ and $B^2(t)$ are independent Brownian motions, and for the function $U = U(\sigma, s)$ then the infinitesimal generator is given by

$$\mathcal{L}U(\sigma, s) = \frac{1}{2}(1-\rho^2)\zeta^2(\sigma)\frac{\partial^2 U}{\partial \sigma^2} + \Gamma(\sigma)\frac{\partial U}{\partial s} + \frac{1}{2}\beta^2(\sigma)\frac{\partial^2 U}{\partial \sigma^2} + v(\sigma)\frac{\partial U}{\partial \sigma},$$

where $\Gamma(\sigma) = \alpha - \dfrac{\zeta^2(\sigma)}{2} - \rho g(\sigma)$. Without any loss of generality, our political risk model discretises volatility σ to $\{\sigma_1, \sigma_2, ..., \sigma_n\}$, and let $\Delta\sigma \equiv \sigma_i - \sigma_{i-1}$. If we now apply our political risk model equation (9) then our transition rate matrix $\mathbf{P}$=(p_{jk}) becomes

$$p_{i,i-1} = \frac{-v(\sigma_i)}{2(\Delta\sigma)} + \frac{\beta^2(\sigma_i)}{2(\Delta\sigma)^2}, p_{i,i+1} = \frac{v(\sigma_i)}{2(\Delta\sigma)} + \frac{\beta^2(\sigma_i)}{2(\Delta\sigma)^2}, p_{i,i} = -\frac{\beta^2(\sigma_i)}{(\Delta\sigma)^2},$$

and $p_{i,j} = 0, \forall |j-i| > 1$. Let us define $U_i = U(s, i\Delta\sigma)$ then we have

$$\frac{\partial U_i}{\partial \sigma} \approx \begin{cases} \dfrac{U_{i+1} - U_i}{\Delta\sigma}, & \text{if } v(\sigma_i) \geq 0 \\ \dfrac{U_{i-1} - U_i}{\Delta\sigma}, & \text{if } v(\sigma_i) < 0, \end{cases} \quad \frac{\partial^2 U_i}{\partial \sigma^2} \approx \frac{U_{i+1} - 2U_i + U_{i-1}}{(\Delta\sigma)^2}. \tag{11}$$

Let

$$\sup_{\sigma\in[\sigma_1,\sigma_n]} |\chi| := \sup_{\sigma\in[\sigma_1,\sigma_n]} \left| \frac{\beta(\sigma_i)}{2}\frac{\partial^2 U_i}{\partial \sigma^2} + v(\sigma_i)\frac{\partial U_i}{\partial \sigma} - [p_{i,i-1}U_{i-1} + p_{i,i}U_i + p_{i,i+1}U_{i+1}] \right|,$$

which can be expressed

$$\begin{aligned}\sup_{\sigma\in[\sigma_1,\sigma_n]} \quad & \Big| \frac{\beta^2(\sigma_i)}{2(\Delta\sigma)^2}\left[U_{i+1} + U_{i-1} - 2U_i - \frac{\partial^2 U_i}{\partial \sigma^2}(\Delta\sigma)^2\right] + \frac{v^+(\sigma_i)}{\Delta\sigma}\left[U_{i+1} - U_i - \frac{\partial U_i}{\partial \sigma}\Delta\sigma\right] \\ - \quad & \frac{v^-(\sigma_i)}{\Delta\sigma}\left[U_{i+1} - U_i - \frac{\partial U_i}{\partial \sigma}\Delta\sigma\right] \Big|. \end{aligned} \tag{12}$$

Hence we have $\sup_{\sigma\in[\sigma_1,\sigma_n]}|\chi| \to 0,\ as\ \Delta\sigma \to 0$. The infinitesimal generator of $(\theta(t), \bar{S}^n(t))$, $\mathcal{L}U_i(s)$, given $\theta(t) = i$, $\bar{S}^n(t) = s$, is given by

$$\mathcal{L}U_i(s) = \frac{1}{2}(1-\rho^2)[\zeta(\sigma_i)]^2\frac{\partial^2 U_i}{\partial s^2} + \Gamma(\sigma_i)\frac{\partial U_i}{\partial s} + \sum_{j=1}^{n} p_{ij}U_j.$$

So by equation (12) we have

$$\mathcal{L}U_i(s) \to \mathcal{L}U_i(s,\sigma_i),\ as\ \Delta\sigma \to 0.$$

Therefore, by applying Theorem 5.1 of (Mijatovic and Pistorius, 2011) we deduce that $(\sigma_{\theta(t)}, \overline{S}^n(t))$ converges weakly to $(\sigma(t), \overline{S}(t))$.

We now consider the jump component. The jump component is statistically independent, so we have

$$\mathbb{E}[\exp(i\xi\tilde{S}(t) + i\sigma_{\theta(t)}\eta)] \quad = \quad \exp(t\gamma(\Phi(\xi)-1))\mathbb{E}[\exp(i\overline{S}^n(t)\xi + i\sigma_{\theta(t)}\eta)].$$

However, from the weak convergence of $(\sigma_{\theta(t)}, \overline{S}^n(t))$ to $(\sigma(t), \overline{S}(t))$, we have

$$\begin{aligned}\exp(t\gamma(\Phi(\xi)-1))\mathbb{E}[\exp(i\overline{S}^n(t)\xi + i\sigma_{\theta(t)}\eta)] &\to \exp(t\gamma(\Phi(\xi)-1))\mathbb{E}[\exp(i\overline{S}(t)\xi + i\sigma(t)\eta)] \\ &= \mathbb{E}[\exp(i\tilde{S}(t)\xi + i\sigma(t)\eta].\end{aligned}$$

Hence $(\sigma_{\theta(t)}, \tilde{S}(t))$ weakly converges to $(\sigma(t), S(t))$. □

The weak convergence is an important result. The result proves that the marginal distributions of our model converge to the values of the original distribution. Therefore the political risk states have a direct relation to the original pricing model. If the political risk states diverged from the original model, then the political risk would differ from the original model and so not provide an accurate model of the political risk.

The weak convergence result is also important from a risk management and measurement perspective. As $(\sigma_{\theta(t)}, \tilde{S}(t))$ weakly converges to $(\sigma(t), S(t))$, the marginal distributions of our model converge to the values of the original distribution. Thus the distributions will not differ, hence any risk measurements or resultant risk management methods will not differ or give misleading results. This is particularly important, given that models have increasingly been scrutinized to ensure that such misleading results do not occur.

The characteristic function provides a full description of the probability function of any model, hence its calculation is an important property for risk measurement. We now derive a recursive method for its calculation.

Lemma 1. *The characteristic function*

$$\mathbb{E}[\exp(i\xi\tilde{Y}^{(M,w)})],\ \textit{where}\ \tilde{Y}^{(M,w)} := \sum_{m=1}^{M} w_m\tilde{h}(\tilde{S}(m)),$$

where $\tilde{h} : \mathbb{R} \to \mathbb{R}$, w_m *is a set of weight* $\forall m \in \{1, 2, ..., M\}$, *and* $\tilde{S}(m) := \log(X(m)/X(m-1))$, *that is the log return of* $X(m)$, *is calculated by recursion.*

Proof. The sequence is initialised with $\tilde{Y}^1 := w_M \tilde{h}(\tilde{S}(M))$. If we assign $\theta(M-1) = j$ then we can initialise the recursion with

$$\begin{aligned}\Phi(\tilde{Y}^1, j, \xi) &= \mathbb{E}_{M-1}[\exp(i\xi\tilde{Y}^1)|\theta(M-1) = j], \\ &= \mathbb{E}_{M-1}[\exp(i\xi w_M \tilde{h}(\tilde{S}(M)))|\theta(M-1) = j], \\ &= \mathbb{E}_{M-1}[\exp(i\xi w_M \tilde{h}(\tilde{S}(\Delta t))|\theta(0) = j].\end{aligned}$$

This can be approximated by integrating against the density function of $\tilde{S}(\Delta t)$ conditional on $\theta(0)$, defined by the characteristic function in the following Corollary.

Corollary 3. *((Buffington and Elliott, 2002)) The characteristic function of* $\tilde{S}(\Delta t)$ *with* n *states, for* $\Delta t > 0$, *is given by*

$$\begin{aligned}\mathbb{E}[\exp(i\tilde{S}(\Delta t)\xi)|\theta(0)] &= \mathbf{1}^{\mathbf{T}}.\exp(\Delta t(\mathbf{P}^{\mathbf{T}} + diag(\psi_1(\xi)) + diag(\psi_2(\xi)) + ... \\ &+ diag(\psi_n(\xi)))\mathbb{I}(0), \text{ for } \mathbf{1} \in \mathbb{R}^n, \mathbb{I}(0) \in \mathbb{R}^n,\end{aligned}$$

where ***1*** *is a unit vector, and* $\mathbb{I}(0)$ *is a vector of zeros except with the value of 1 at the position of* $\theta(0)$.

A direct application of the Corollary gives

$$\begin{aligned}&\mathbb{E}[\exp(i\xi\tilde{S}(\Delta t))|\theta(0) = j] \\ = &\sum_{k=1}^{n} \mathbb{E}[exp(i\xi\tilde{S}(\Delta t))|\theta(0) = j, \theta(\Delta t) = k]exp(i\xi\tilde{h}(\sigma_k, \sigma_j))\end{aligned}$$

To determine sequences $m \in \{2, .., M\}$, if we define

$$p(j, k, \Delta t) = \mathbb{P}(\theta(t + \Delta t) = k|\theta(t) = j], \tag{13}$$

$$H(j, k) = \{\theta(0) = j, \theta(\Delta t) = k\}, \tag{14}$$

then the remaining sequences can be obtained by

$$\begin{aligned}\Phi(\tilde{Y}^m, j, \xi) &= \mathbb{E}[\exp(i\xi\tilde{Y}^m)|\theta(M-m) = j] \\ &= \mathbb{E}[\exp(i\xi w_{M-m+1}\tilde{h}(\tilde{S}(M-m+1)))\exp(i\xi\tilde{Y}_{m-1}|\theta(M-m) = j], \\ &= \sum_{k=1}^{n} \mathbb{E}_{M-m}[\exp(i\xi w_{M-m+1}\tilde{h}(\tilde{S}(M-m+1)))|\theta(M-m) = j, \\ &\quad \theta(M-(m-1)) = k] \cdot p(j, k, \Delta t), \\ &= \sum_{k=1}^{n} \mathbb{E}_{M-m}[\exp(i\xi w_{M-m+1}\tilde{h}(\tilde{S}(M-m+1)))|H(j, k)] \\ &\quad \cdot\mathbb{E}_{M-m}[\exp(i\xi\tilde{Y}_{m-1}|\theta(N-m) = j, \theta(M-(m-j)) = k] \cdot p(j, k, \Delta t), \\ &= \sum_{k=1}^{n} \mathbb{E}[\exp(i\xi w_{M-m+1}\tilde{h}(\tilde{S}(\Delta t))|H(j, k)] \cdot p(j, k, \Delta t).\Phi(\tilde{Y}^{m-1}, k, \xi).\end{aligned}$$

In the last line $\Phi(\tilde{Y}^{m-1}, k, \xi)$ is the conditional characteristic function of $\tilde{Y}^{m-1}$ and this is know at stage m; note that $\Phi(\tilde{Y}^{m-1}, k, \xi) = \mathbb{E}_{M-m}[exp(i\xi\tilde{Y}_{m-1})|\theta(M-m) = j, \theta(M-(m-1)) = k]$. To obtain $\mathbb{E}[\exp(i\xi w_{M-m+1}\tilde{h}\tilde{S}(\Delta t))|H(j,k)]$ in $\forall j,k \in \{1,2,...,n\}$ conditional on $\theta(0)$ and $\theta(\Delta t)$, one integrates densities of $\tilde{S}(\Delta t)$ and these are determined by their characteristic functions

$$\begin{aligned}\mathbb{E}[\exp(i\xi\tilde{S}(\Delta t)|H(j,k)] &= \left(\frac{1}{p(j,k,\Delta t)}\right)\cdot\mathbb{E}[\exp(i\xi\tilde{S}(\Delta t))|\theta(0)=j,\theta(\Delta t)=k] \\ &\quad\cdot\exp(i\xi\tilde{h}(\sigma_k,\sigma_j)).\end{aligned}$$

Now we define $p(y|s,j,k)$ as the density of $\tilde{S}(\Delta t)$ conditional on $H(j,k)$ as

$$p(y|s,j,k) = \mathbb{P}(\tilde{S}(\Delta t) \in y + dy|\tilde{S}(0) = s, \theta(0) = j, \theta(\Delta t) = k). \tag{15}$$

Whilst $p(y|s,j,k) = p(y-s,j,k)$ has no closed form solution, it can be found using $\mathbb{E}[\exp(i\xi\tilde{S}(\Delta t)|H(j,k)]$ and Fourier transform methods. We will use the PROJ method (see later). □

To give an application we derive the discretely sampled variance characteristic function for $w_m = 1$ and $\tilde{h}(s) = s^2$:

$$\Phi_{\tilde{Y}_M}(\xi) := \mathbb{E}\left[\exp\left(\mathrm{i}\xi\sum_{m=1}^{M}\tilde{S}^2(m)\right)\right] = \mathbb{E}\left[\exp\left(\mathrm{i}\xi\tilde{Y}_M\right)\right], \quad \tilde{Y}_M := \sum_{m=1}^{M}\tilde{S}^2(m). \tag{16}$$

The recursion is derived to be

$$\tilde{Y}_1 := \tilde{h}(\tilde{S}(m)), \quad \tilde{Y}_m := \tilde{h}(\tilde{S}(M-(m-1))) + \tilde{Y}_{m-1}, \quad m = 2,\ldots,M. \tag{17}$$

Once $\Phi^j_{\tilde{Y}_1}(\xi) = \mathbb{E}[e^{\mathrm{i}\xi\tilde{h}(\tilde{S}(\Delta t))}|\theta(0)=j] = \sum_{k=1,..,n}\hat{\Phi}_{j,k}(\xi)$ is known, then

$$\Phi^j_{\tilde{Y}_m}(\xi) = \sum_{k=1,..,n}\hat{\Phi}_{j,k}(\xi)\cdot\Phi^k_{\tilde{Y}_{m-1}}(\xi), \quad m = 2,\ldots,M, \tag{18}$$

and we have

$$\hat{\Phi}_{j,k}(\xi) := p(j,k,\Delta t)\cdot\mathbb{E}[\exp(\mathrm{i}\xi\tilde{h}(\tilde{S}(\Delta t))|H(j,k)], \quad j,k = 1,\ldots,n. \tag{19}$$

5 Political Risk Measurement

In this section we provide a method to measure political risk, which is achieved using the biorthogonal projection method (PROJ). The PROJ is applied to risk measures and our political risk model. This enables us to derive some risk measures for political risk.

5.1 Biorthogonal Projection

It was previously mentioned that $p(y|s,j,k)$, the density of $\tilde{S}(\Delta t)$ conditional on $H(j,k)$, has no closed form solution, it can be found using Fourier transform methods. The Biorthogonal Projection method (PROJ) introduced in (Kirkby, 2015) is a Fourier transform method. The orthogonal projection onto an appropriately chosen basis provides the probability density of a random variable.

Let us assume we have a random variable Q with an unknown probability density f_Q, and that its characteristic function $\Phi_Q(\xi)$ is known, or can be approximated. If we have a compactly supported *generator* $\varphi(q)$, a *resolution* $a > 0$, and a reference point q_1, then we specify the basis elements set

$$\varphi_{a,\hat{m}}(q) := a^{1/2}\varphi(a(q - q_{\hat{m}})).$$

We say that the orthogonal projection $P_{\mathcal{M}_a} f_Q$ of f_Q onto $\mathcal{M}_a := \overline{\text{span}}\{\varphi_{a,\hat{m}}\}_{\hat{m}\in\mathbb{Z}}$ is determined by the *dual basis* $\{\widetilde{\varphi}_{a,\hat{m}}\}_{\hat{m}\in\mathbb{Z}}$, which is given by

$$P_{\mathcal{M}_a} f_Q(q) = \sum_{\hat{m}\in\mathbb{Z}} \langle f_Q, \widetilde{\varphi}_{a,\hat{m}}\rangle \varphi_{a,\hat{m}}(q),$$

where the dual basis is *biorthogonal* in that $\langle \varphi_{a,k}, \widetilde{\varphi}_{a,\hat{m}}\rangle = \mathbb{1}_{\{k=\hat{m}\}}$, as well as the particular case of an orthogonal basis is self-dual. To determine the projection coefficients, these are derived in closed-form using the Fourier transform $\widehat{\widetilde{\varphi}}$ of $\widetilde{\varphi}$:

$$\langle f_Q, \widetilde{\varphi}_{a,\hat{m}}\rangle = \frac{a^{-1/2}}{\pi} \Re\left[\int_0^\infty \exp(-\mathrm{i}q_{\hat{m}}\xi)\cdot \Phi_Q(\xi)\widehat{\widetilde{\varphi}}\Big(\frac{\xi}{a}\Big) d\xi\right], \tag{20}$$

assuming that $\widehat{\widetilde{\varphi}}(\xi)$ is known. Additionally, we will use the cubic B-spline generator in our paper

$$\varphi(y) = \begin{cases} (y+2)^3/6, & y\in[-2,-1] \\ 2/3 - y^3/2 - y^2, & y\in[-1,0] \\ 2/3 + y^3/2 - y^2, & y\in[0,1] \\ (2-y)^3/6, & y\in[1,2]. \end{cases} \tag{21}$$

Given that we have fixed a, N and q_1, we constrain $\mathcal{M}_a$ to a finite set $\{q_{\hat{m}}\}_{\hat{m}=1}^N$ and each basis element $\varphi_{a,\hat{m}}(q)$ will be centered over the grid point $q_{\hat{m}} = q_1 + (\hat{m}-1)/a$. Accounting for the Nyquist frequency, we specify an N-point frequency grid

$$\Delta_\xi = 2\pi a/N, \qquad \xi_{\hat{m}} = (\hat{m}-1)\Delta_\xi, \quad \hat{m} = 1,...,N, \tag{22}$$

and this is numerically applied to invert the analytical coefficient representation in equation (20). Therefore our final approximation is defined by

$$f_Q(q) \approx a^{1/2}\Upsilon_{a,N} \sum_{1\le k\le N} \bar{\beta}_{a,k}\cdot\varphi_{a,k}(q),$$

where we have the constant $\Upsilon_{a,N} := 32a^4/N$. Additionally, the coefficients $a^{1/2}\Upsilon_{a,N} \cdot \bar{\beta}_{a,k} \approx \tilde{\beta}_{a,k} = \langle f_Q, \widetilde{\varphi}_{a,k} \rangle$ are determined by the exponentially convergent discretization

$$\left\{\bar{\beta}_{a,k}\right\}_{k=1}^{N} := \Re\left\{\mathcal{D}\left\{G_j\right\}\right\}, \quad \mathcal{D}_n\left\{G_j\right\} = \sum_{j=1}^{N} e^{-\mathrm{i}\frac{2\pi}{N}(j-1)(\hat{m}-1)} G_j, \quad \hat{m} = 1, ..., N, \tag{23}$$

and the discrete Fourier transform (DFT) is denoted by the operator $\mathcal{D}\{.\}$. The set $\{G_j\}_{j=1}^{N}$, which is referred to as the DFT input vector, is also specified by

$$G_1 := 1/32a^4, \qquad G_{\hat{m}} := \Phi_Q(\xi_{\hat{m}}) \cdot \mathcal{B}_{\hat{m}} \cdot \exp(-\mathrm{i}\xi_{\hat{m}} \cdot q_1), \quad \hat{m} \geq 2, \tag{24}$$

where

$$\mathcal{B}_{\hat{m}} := \frac{2520(\sin(\xi_{\hat{m}}/(2a))/\xi_{\hat{m}})^4}{1208 + 1191\cos(\xi_{\hat{m}}/a) + 120\cos(2\xi_{\hat{m}}/a) + \cos(3\xi_{\hat{m}}/a)}, \quad \hat{m} \geq 2. \tag{25}$$

For details on the derivation of $\widehat{\widetilde{\varphi}}$ (and $\mathcal{B}_{\hat{m}}$) for B-spline bases, the reader is referred to (Kirkby, 2017).

Remark 1. *Using the log return process in the regime-switching model, the truncated density support parameter $\mathcal{Z}$ is derived on generic rules relating to cumulants. For the regime switching model, the jump and diffusion processes are independent, we have the characteristic exponent defined by*

$$\psi_j(\xi) = i\xi\alpha(j) - \frac{\xi^2\tilde{\sigma}^2(j)}{2} + \gamma(\Phi(\xi) - 1), \quad \forall j \in \mathcal{S}.$$

We define the i^{th} cumulant of the jump component as c_i^{λ}, where the jump types modeled in this paper are given in Table 1. Specifically, we consider typical jump types with Normal distributions, double exponential distributions (DE) and mixed Normal distributions. We note in passing that the jumps have intensity γ, the characteristic exponent of the jump contribution is $\gamma(\Phi(\xi) - 1)$, also $\iota := \Phi(-i) - 1$, and $\gamma\iota$ is the drift compensator.

Jump Type	$\nu(y)$	$\Phi(\xi)$
Normal	$\frac{1}{\sqrt{2\pi}b_1} e^{-(q-a_1)^2/2b_1^2}$	$e^{\mathrm{i}\xi a_1 - \frac{1}{2}\xi^2 b_1^2}$
DE	$p\eta_1 e^{-\eta_1 y}\mathbb{I}_{\{y\geq 0\}} + (1-p)\eta_2 e^{\eta_2 y}\mathbb{I}_{\{y<0\}}$	$p\frac{\eta_1}{\eta_1 - \mathrm{i}\xi} + (1-p)\frac{\eta_2}{\eta_2 + \mathrm{i}\xi}$
Mixed Normal	$p\frac{1}{\sqrt{2\pi}b_1} e^{-\frac{(y-a_1)^2}{2b_1^2}} + (1-p)\frac{1}{\sqrt{2\pi}b_2} e^{-\frac{(y-a_2)^2}{2b_2^2}}$	$pe^{\mathrm{i}\xi a_1 - \frac{1}{2}\xi^2 b_1^2} + (1-p)e^{\mathrm{i}\xi a_2 - \frac{1}{2}\xi^2 b_2^2}$

Table 1: Jump types specified by Lévy measure $\nu(y)$ and characteristic function $\Phi(\xi)$ for common jump distributions

We devise a grid, that is an alternative to the (Fang and Oosterlee, 2009) method, and is specified by

$$\bar{\mathcal{Z}} = \max\left\{\frac{1}{2},\ L_1 \cdot \sqrt{c_2^* T + \sqrt{c_4^* T}}\right\}, \quad c_2^* := c_2^{\lambda} + \zeta^2(\bar{\eta}(T/2)), \quad c_4^* := c_4^{\lambda},$$

with $L_1 = 10 \sim 14$. The diffusion component's second cumulant is specified by $\zeta(\sigma)$ and $\bar{\mu}(t) = \bar{\eta}$ (as defined earlier).

Jump Type	c_2^λ	c_4^λ
Normal	$\gamma(a_1^2+b_1^2)$	$\gamma(a_1^4+6b_1^2a_1^2+3b_1^4\gamma)$
DE	$2\gamma\left(\frac{p}{\eta_1^2}+\frac{(1-p)}{\eta_2^2}\right)$	$24\gamma\left(\frac{p}{\eta_1^4}+\frac{1-p}{\eta_2^4}\right)$
Mixed Normal	$p\gamma(a_1^2+b_1^2)+(1-p)\gamma(a_2^2+b_2^2)$	$p\gamma(a_1^4+6b_1^2a_1^2+3b_1^4\gamma)+(1-p)\gamma(a_2^4+6b_2^2a_2^2+3b_2^4\gamma)$

Table 2: Cumulants of common jump distributions (defined in Table 1).

We require an approximation for Ψ and we utilise the Gaussian quadrature, over each interval $I_k=[q_k-2\Delta,q_k+2\Delta]$, $k=1,\ldots,N$. By applying a change of variables, this is achieved by using an N_q-point quadrature for every subinterval in $[-2,2]=[-2,-1]\cup[-1,0]\cup[0,1]\cup[1,2]$ as follows. Specifically,

$$\begin{aligned}\Psi(\hat{m},k) &:= \Upsilon_{a,N}\cdot a^{1/2}\int_{I_k}\exp(\mathrm{i}\xi_{\hat{m}}\tilde{h}(q))\cdot a^{1/2}\varphi(a(y-q_k))dy\\ &= \Upsilon_{a,N}\int_{[-2,2]}\exp\left(\mathrm{i}\xi_{\hat{m}}h\left(q_k+\frac{y}{a}\right)\right)\varphi(y)dy\\ &\approx \Upsilon_{a,N}\sum_{l=1}^{4\cdot N_q}\omega_l\cdot\exp\left(\mathrm{i}\xi_{\hat{m}}h\left(q_k+\hat{\omega}_l\right)\right)\varphi(\hat{\omega}_l),\end{aligned}$$

where $\{(\hat{\omega}_l,\omega_l)\}_{l=1}^{4\cdot N_q}$ are the nodes and weights on $[-2,2]$. We then specifiy a sample grid

$$\eta_j,\quad j=1,...,N_\eta,\qquad N_\eta:=((N-1)+4)\cdot N_q, \tag{26}$$

where η_j is a refined grid over $q_1-2\Delta,\ldots,q_N+2\Delta$, hence subintervals with length Δ have N_q points from the group $\{\eta_j\}_{j=1}^{N_\eta}$. We note in passing that $(N-1)+4$ such intervals exist.For $\Psi(\hat{m},k)$, the Gaussian approximation for $\hat{m}=1,\ldots,N$ and $k=1,\ldots,N$, is defined by

$$\bar{\Psi}(\hat{m},k):=\sum_{l=1}^{4\cdot N_q}\theta^{\hat{m}}_{N_q(k-1)+l}\cdot e_l=\sum_{l=1}^{2\cdot N_q}\left(\theta^{\hat{m}}_{N_q(k-1)+l}+\theta^{\hat{m}}_{N_q(k+3)+1-l}\right)\cdot e_l, \tag{27}$$

where

$$e_l:=\Upsilon_{a,N}\cdot\varphi(\hat{\omega}_l)\cdot\omega_l,\quad l=1,...,2\cdot N_q,$$

and

$$\theta_j^n:=\exp\left(\mathrm{i}\xi_n\tilde{h}(\eta_j)\right),\qquad n=1,...,N,\quad j=1,...,N_\eta.$$

This is applied in Remark 2 with $N_q=5$ point Gaussian quadrature, so each basis element $\varphi_{a,k}(q)$ is integrated against $\exp(i\xi\tilde{h}(q))$ using a total of $4\cdot N_q=20$ points.

Remark 2. *To integration of $\Psi(\hat{m},k)$ is calculated numerically by using a composite Gaussian quadrature with a five point rule, and this is applied over each interval $[\tilde{r},\tilde{r}+1]$, for $\tilde{r}\in\{-2,-1,0,1\}$. If we consider the symmetry of $\varphi(y)$, then it can be deduced that we only require the nodes $\{\hat{\omega}_l\}$ and weights $\{\omega_l\}$ for $\tilde{r}\in\{-2,-1\}$ (see equation (27)). For the region $[-2,-1]$, we have*

$$\{\hat{\omega}_l\}_{l=1}^5=\Big\{-\frac{3}{2}-g_3,-\frac{3}{2}-g_2,-\frac{3}{2},-\frac{3}{2}+g_2,-\frac{3}{2}+g_3\Big\},\quad \{\omega_l\}_{l=1}^5=\frac{1}{2}\{v_3,v_2,v_1,v_2,v_3\},$$

and on the region $[-1,0]$ *we have*

$$\{\hat{\omega}_l\}_{l=6}^{10} = \Big\{ -\frac{1}{2} - g_3, -\frac{1}{2} - g_2, -\frac{1}{2}, -\frac{1}{2} + g_2, -\frac{1}{2} + g_3 \Big\}, \quad \{\omega_l\}_{l=6}^{10} = \frac{1}{2}\{v_3, v_2, v_1, v_2, v_3\},$$

where the constants are specified by $g_2 := \frac{1}{6}(5 - 2\sqrt{10/7})^{1/2}$, $g_3 := \frac{1}{6}(5 + 2\sqrt{10/7})^{1/2}$, $v_1 := 128/225$, $v_2 := (322 + 13\sqrt{70})/900$, $v_3 := (322 - 13\sqrt{70})/900$. *Moreover,* $e_l = \Upsilon_{a,N} \cdot \varphi(\hat{\omega}_l) \cdot w_l$ *are the final set of weights and are determined by evaluating the cubic generator* $\varphi(y)$ *defined in equation* (21) *at each of* $\{\hat{\omega}_l\}_{l=1}^{10}$. *We note that we store* e_l *for repeated use.*

5.2 Political Risk Model Calculation

The characteristic function was previously defined by recursion, ending with $\Phi^j_{\hat{Y}_M}(\xi)$. We derive our characteristic function calculation by firstly analysing equations for $2 \leq m \leq M$, where the fundamental calculation is the characteristic function $\Phi^j_{\hat{Y}_m}(\xi)$, and determining $\hat{\Phi}_{j,k}$ in equation (19). The conditional transition density in equation (15) is reformulated by its orthogonal projection onto the cubic basis, that is

$$\begin{aligned} p(\nu|j,k) &\approx \sum_{\hat{m}\in\mathbb{Z}} \left(\int_{-\infty}^{\infty} p(\eta|j,k) \widetilde{\varphi}_{a,\hat{m}}(\eta) d\eta \right) \varphi_{a,\hat{m}}(\nu) \\ &= \frac{a^{-1/2}}{\pi} \frac{1}{p(j,k,\Delta t)} \sum_{\hat{m}\in\mathbb{Z}} \Re \left\{ \int_0^{\infty} \exp(-i\nu_{\hat{m}}\xi) \cdot \widetilde{\mathcal{E}}_{k,j}(\xi) \cdot \widehat{\widetilde{\varphi}}(\xi/a) d\xi \right\} \varphi_{a,\hat{m}}(\nu), \end{aligned} \tag{28}$$

where $\widetilde{\mathcal{E}} = \mathbb{E}[\exp(i\tilde{S}(\Delta t)\xi)|\theta(0) = j, \theta(\Delta t) = k]$ as in section 4. The number of basis elements N is set at a constant (for instance $N = 2^{10}$), the grid width parameter $\bar{\mathcal{Z}} \in \mathbb{R}$ is determined as described in Remark 1, we define a common grid for the density projections by

$$\Delta = 2\bar{\mathcal{Z}}/(N-1), \quad s_1 = (1 - N/2)\Delta, \quad s_{\hat{m}} = s_1 + (\hat{m} - 1)\Delta, \quad \hat{m} = 1, \ldots, N,$$

where $a = 1/\Delta$, and the frequency grid $\{\xi_{\hat{m}}\}_{\hat{m}=1}^N$ is obtained from equation (22). We discretize the analytical formula in equation (28) by

$$p(j,k,\Delta t) \cdot p(\nu|j,k) \approx a^{1/2} \Upsilon_{a,N} \sum_{1\leq l\leq N} \bar{\beta}^{j,k}_{a,l} \cdot \varphi_{a,l}(\nu) =: \bar{p}(\nu|j,k),$$

where $\left\{ \bar{\beta}^{j,k}_{a,l} \right\}_{l=1}^N := \Re \left\{ \mathcal{D} \left\{ G^{j,k}_{\hat{m}} \right\} \right\}$ and is obtained from the DFT input vector

$$G^{j,k}_1 := \widetilde{\mathcal{E}}_{k,j}(\xi_1)/32a^4, \qquad G^{j,k}_{\hat{m}} := \widetilde{\mathcal{E}}_{k,j}(\xi_{\hat{m}}) \cdot \zeta_{\hat{m}} \cdot \exp(-\mathrm{i}\xi_{\hat{m}} \cdot s_1), \quad \hat{m} \geq 2, \tag{29}$$

with $\mathcal{B}_{\hat{m}}$ specified by equation (25). If we have a representation of the transition densities between each state, using $\{\xi_{\hat{m}}\}_{\hat{m}=1}^N$ the conditional characteristic function of $\tilde{h}(\tilde{S}(\Delta t))$ can be derived.

The function $\hat{\Phi}(\xi_{\hat{m}})$ for each $\xi_{\hat{m}}$ is approximated by $\bar{\Phi}(\xi_{\hat{m}}) = \{\bar{\Phi}_{j,k}(\xi_{\hat{m}})\}_{j,k=1}^{n}$ and this is derived by

$$\begin{aligned}
\hat{\Phi}_{j,k}(\xi_{\hat{m}}) &= p(j,k,\Delta t) \cdot \mathbb{E}[\exp(\mathrm{i}\xi_{\hat{m}}\tilde{h}(\tilde{S}(\Delta t))|G_{jk}] \\
&= p(j,k,\Delta t) \int_{-\infty}^{\infty} e^{\mathrm{i}\xi_{\hat{m}}\tilde{h}(s)} p(s|j,k) ds \\
&\approx \Upsilon_{a,N} \sum_{1\le l\le N} \bar{\beta}_{a,l}^{j,k} \cdot a^{1/2} \int_{-\infty}^{\infty} e^{\mathrm{i}\xi_{\hat{m}}\tilde{h}(s)} \varphi_{a,l}(s) ds \\
&= \Upsilon_{a,N} \sum_{1\le l\le N} \bar{\beta}_{a,l}^{j,k} \Psi_{\hat{m},l} \\
&= \Psi_{(\hat{m},\cdot)} B^{j,k} =: \bar{\Phi}_{j,k}(\xi_{\hat{m}}),
\end{aligned} \tag{30}$$

where $B_l^{j,k} := \bar{\beta}_{a,l}^{j,k}$ and Ψ represents the matrix of integrals

$$\Psi_{\hat{m},l} = \Upsilon_{a,N} \cdot a^{1/2} \int_{-\infty}^{\infty} e^{\mathrm{i}\xi_{\hat{m}}\tilde{h}(s)} \varphi_{a,l}(s) ds, \quad \hat{m}, l = 1, \ldots, N.$$

We also have $\bar{\Phi}_{j,k} = \Psi B^{j,k}$, and obtaining $\bar{\Phi}_{j,k}$, implies that the sequence of $\Phi^j_{\tilde{Y}_m}(\xi_{\hat{m}})$ for $m = 2, \ldots, M$ satisfies equation (18). We now require $\Phi^j_{\tilde{Y}_m}(\xi_{\hat{m}})$ for $m = 1$, that is the initialization or $\Phi^j_{\tilde{Y}_1}(\xi)$. This derived by

$$\begin{aligned}
\Phi^j_{\tilde{Y}_1}(\xi) &= \sum_{k=1,..,n} \mathbb{E}[\mathbb{1}_{\{\alpha(\Delta_t)=k\}} \cdot \exp(\mathrm{i}\xi\tilde{h}(\tilde{S}(\Delta t)))|\theta(0) = j] \\
&= \sum_{k=1,..,n} \hat{\Phi}_{j,k}(\xi),
\end{aligned} \tag{31}$$

which is approximated by replacing $\hat{\Phi}$ with $\bar{\Phi}$.

Once we have obtained the set $\{\Phi^j_{\tilde{Y}_M}(\xi)\}_{j=1}^{n}$, we obtain the variance states, indexed by k_0 and k_{0+1} such that $\sigma_{k_0} \le \sigma_0 < \sigma_{k_0+1}$, given σ_0. Using a grid $\{y_{\hat{m}}\}_{\hat{m}=1}^{N/2}$ for $\tilde{Y}_M$ we can then obtain the density coefficients for $\Phi^j_{\tilde{Y}_M}(\xi)$ over $j \in \{k_0, k_0+1\}$, which we denote by $\{\hat{\beta}^j_{a,\hat{m}}\}_{\hat{m}=1}^{N}$. They are determined by the FFT as in equation (23), where the input for $j \in \{k_0, k_0+1\}$ is

$$G_1^j := 1/32a^4, \qquad G_{\hat{m}}^j := \Phi^j_{\tilde{Y}_M}(\xi_{\hat{m}}) \cdot \mathcal{B}_{\hat{m}} \cdot \exp(-\mathrm{i}\xi_{\hat{m}} \cdot y_1), \quad \hat{m} \ge 2, \tag{32}$$

with $\xi_{\hat{m}}$ defined in equation (22) and $\mathcal{B}_{\hat{m}}$ in (25).

The final calculation for risk measurement is dependent on the risk measure function $\tilde{\rho}(.)$ itself, where $\tilde{\rho}(.)$ denotes some risk measure (to be explained in more detail later). A risk measure is commonly a function of expectation $\mathbb{E}[.]$, hence our risk measure would be expressed as

$$\mathbb{E}[f(\tilde{Y}_M)] \approx \mathcal{A}^{k_0} + (\mathcal{A}^{k_0+1} - \mathcal{A}^{k_0}) \frac{\sigma_0 - \sigma_{k_0}}{\sigma_{k_0+1} - \sigma_{k_0}}$$

where

$$\mathcal{A}^j := \Upsilon_{a,N} \sum_{\hat{m}=1}^{N/2} \hat{\beta}^j_{a,\hat{m}} \Theta^{\alpha}_{\hat{m}}, \quad j = k_0, k_0+1,$$

and

$$\Theta^{\alpha}_{\hat{m}} := a^{1/2} \int_0^{\infty} \varphi_{a,\hat{m}}(y) f(y) dy.$$

For instance, for upside risk measurement (to be discussed in the proceeding sections) with respect to threshold K, we have

$$\tfrac{1}{T}\mathbb{E}[(\tilde{Y}_M - KT)^+].$$

The grid is defined by $y_1 = KT - \Delta$, $y_{\hat{m}} = y_1 + (n-1)\Delta$ for $\hat{m} = 1, \ldots, N/2$, and

$$\Theta_{\hat{m}} = \begin{cases} (y_{\hat{m}} - KT)/24 + \Delta/20 & \hat{m} = 1 \\ (y_{\hat{m}} - KT)/2 + \Delta \cdot 7/30 & \hat{m} = 2 \\ (y_{\hat{m}} - KT) \cdot 23/24 + \Delta/20 & \hat{m} = 3 \\ (y_{\hat{m}} - KT) & \hat{m} = 4, \ldots, N/2, \end{cases} \tag{33}$$

where $y_{\hat{m}} - KT = -\Delta + (\hat{m} - 1)\Delta$.

5.3 Risk Measurement

The fundamental work of (Artzner et al., 2003) has led to axiomatic definitions in measuring risk. Risk measurement is defined as some functional on the sample space of losses. Let us assume we have a real valued random variable $X \in \mathbb{R}$ within the measurable space $\{\Omega, \mathcal{F}\}$, where X follows a distribution of losses $\mathcal{G}$, then a risk measure $\tilde{\rho}$ is defined by

$$\tilde{\rho} : \mathcal{G} \mapsto \mathbb{R}.$$

In particular, we consider a risk measure is capable of measuring risk correctly (or "coherently") if the risk measure conforms to the coherency axioms (Artzner et al., 2003), that is translation invariance, subaddivity, monotonicity and positive homogeneity and are given (respectively) as

$$\begin{aligned} \tilde{\rho}(X + k) &= \tilde{\rho}(X) + k, \text{ for } k \in \mathbb{R}, \\ \tilde{\rho}(X_1 + X_2) &\leq \tilde{\rho}(X_1) + \tilde{\rho}(X_2), \\ \tilde{\rho}(X_1) &\leq \tilde{\rho}(X_2), \forall X_1 \leq X_2, \\ \tilde{\rho}(kX) &= k\tilde{\rho}(X), \forall k \in \mathbb{R}_{\geq 0}. \end{aligned}$$

Whilst it is known that volatility is not directly observable in markets, the realized variance (a standard measure for volatility) is directly observable for assets and is given by

$$\Lambda_M = \frac{1}{T} \sum_{m=1}^{M} \left(\log \frac{X(t_m)}{X(t_{m-1})} \right)^2.$$

Given that Λ_M changes over time t, we will obtain a distribution of values for Λ_M. Let us denote the random variable that generates this distribution as $\tilde{\Lambda}_M$, hence we can empirically measure political risk using $\tilde{\rho}(\tilde{\Lambda}_M)$.

Using our PROJ method and previous theorems, we are now in a position to calculate risk using risk measures. Once the characteristic function of realized variance has been recovered, we can calculate various risk measures after inverting to obtain a density. For this purpose, it is convenient to utilize a lower order B-spline basis, namely the linear B-splines with generator

$$\varphi(y) = (1+y)\mathbb{1}_{[-1,0]}(y) + (1-y)\mathbb{1}_{[0,1]}(y).$$

Let $\tilde{Y}_M := T \cdot \Lambda_M$, for which we will recover the terminal density. To recover the terminal density, we specify a grid of points $y_n = (n-1)\Delta$, $n = 1, \ldots, N/2$, where $\Delta := 1/a$, and note that $y_1 = 0$ as the density for realized variance is defined over $[0, \infty)$. Define the DFT input vector $\{G_j^{[1]}\}_{j=1}^N$ by

$$G_1^{[1]} := 1/24a^2, \qquad G_m^{[1]} := \Phi_{Y_M}(\xi_m) \cdot \mathcal{B}_m^{[1]}, \quad m \geq 2, \tag{34}$$

where ξ_m is defined in (22), and

$$\mathcal{B}_m^{[1]} := \frac{(\sin(\xi_m/(2a))/\xi_m)^2}{2 + \cos(\xi_m/a)}, \quad m \geq 2. \tag{35}$$

The final density is approximated by

$$f_{\tilde{Y}_M}(y) \approx a^{1/2}\Upsilon_{a,N}^{[1]} \sum_{1 \leq \hat{m} \leq N/2} \bar{\beta}_{a,\hat{m}}^{[1]} \cdot \varphi_{a,\hat{m}}(y),$$

where $\Upsilon_{a,N}^{[1]} := 24a^2/N$, and $\bar{\beta}_{a,k}^{[1]}$ are obtained using the DFT defined in (23), but with input vector $\{G_m^{[1]}\}_{m=1}^N$. In general, to avoid boundary effects in the computation of the DFT, we will only require the density for the grid points $\{y_n\}_{n=1}^{N/2}$. Once $f_{\tilde{Y}_M}(y)$ is recovered over $\{y_{\hat{m}}\}_{\hat{m}=1}^{N/2}$, a range of risk measures can be computed.

The variety of risk measures that currently exist in the literature is diverse, see (Szegö, 2005) for a review of risk measures. A popular risk measure is Value at Risk (VaR) which is defined as

$$VaR(X) = \inf\{x \in \mathbb{R} : \mathbb{P}(X \leq x) \geq \hat{\alpha}\},$$

such that $\{\hat{\alpha} \in \mathbb{R}_{\geq 0} | 0 \leq \hat{\alpha} \leq 1\}$. Essentially, an individual specifies a confidence level (or risk level) $\hat{\alpha}$ and the associated threshold value is given by VaR, where typically $\hat{\alpha} \in \{0.90, 0.95, 0.99\}$. For our realised variance then VaR measure equates to

$$VaR(\tilde{\Lambda}_M) = \inf\{k \in \mathbb{R} : \mathbb{P}(\tilde{\Lambda}_M \leq k) \geq \hat{\alpha}\},$$

for some given k.

Let $\bar{\beta}_{a,n} := \bar{\beta}_{a,n}^{[1]}$. To calculate VaR, we take advantage of one of the nice properties of the linear basis. In particular, define the cumulative distribution approximation, which is calculated at the grid points calculated at the grid points $y_{\hat{m}} = \{(\hat{m}-1)\Delta\}_{\hat{m}=1}^{N/2}$ using using

$$\bar{F}_{\hat{m}} := \bar{F}(y_{\hat{m}}) = a^{-1/2} \sum_{j=1}^{\hat{m}-1} \bar{\beta}_{a,j} + \frac{a^{-1/2}}{2} \bar{\beta}_{a,\hat{m}}, \tag{36}$$

and define the boundary coefficients $\bar{\beta}_{a,0} = \bar{\beta}_{a,N/2+1} = 0$. We can then calculate the distribution at any $y \in [0, \infty)$ using

$$\bar{F}(y) = \bar{F}(y_{\hat{m}}) + a^{-1/2}\left[\mathcal{B}\bar{\beta}_{a,\hat{m}} + \frac{\mathcal{B}^2}{2}\left(\bar{\beta}_{a,\hat{m}+1} - \bar{\beta}_{a,\hat{m}}\right)\right],$$

$\mathcal{B} := a(y - y_{\hat{m}})$, and is defined as $F(y) = 1$ for $y > y_{N/2}$. For any VaR level, $p \in (0,1)$, let $k \in \{0 \ldots, N/2\}$ be the unique integer satisfying $\bar{F}_k \leq U < \bar{F}_{k+1}$, and set $d_k := \bar{\beta}_{a,k+1} - \bar{\beta}_{a,k}$. We then have the closed form expression for VaR,

$$VaR(p) = T^{-1} \cdot \begin{cases} y_k + \dfrac{1}{a \cdot d_k}\left(-\bar{\beta}_{a,k} + \sqrt{\bar{\beta}_{a,k}^2 + 2a^{1/2} \cdot d_k(p - \bar{F}_k)}\right), & d_k \neq 0; \\ y_k + \dfrac{p - \bar{F}_k}{a \cdot (\bar{F}_{k+1} - \bar{F}_k)}, & d_k = 0. \end{cases} \tag{37}$$

Another popular risk measure is taking the moments of a random variable , that is our risk measure

$$\tilde{\rho}(\tilde{\Lambda}_M) = \mathbb{E}[\tilde{\Lambda}_M^k],$$

is the k^{th} moment, for $k \in \mathbb{N}^+$. The moment measure of risk is a convenient measure, and moments provide useful information about the distribution of random variables. Hence such moments enable us to understand the risk of $\tilde{\Lambda}_M$. In particular the second central moment or variance

$$\tilde{\rho}(\tilde{\Lambda}_M) = Var(\tilde{\Lambda}_M),$$

where $Var(.)$ is the variance of the random variable, has been in existence as a risk measure for many decades. It is frequently used in risk optimization of portfolios using Markowitz Portfolio Theory (Markowitz, 1952), and it is a coherent risk measure, hence measures risk correctly.

To measure risk using moments we first approximate the moments, for $k \geq 1$,

$$\mathbb{E}[\tilde{\Lambda}_M^k] = T^{-k} \cdot \mathbb{E}[Y_M^k] \approx \Upsilon_{a,N}^{[1]} \sum_{1 \leq \hat{m} \leq N/2} \bar{\beta}_{a,\hat{m}}^{[1]} \Theta_{\hat{m}}^{(k)}, \tag{38}$$

where $\Theta_{\hat{m}}^{(k)}$ are given by the formula

$$\Theta_{\hat{m}}^{(k)} = T^{-k} \cdot \begin{cases} z_a(k), & \hat{m} = 1 \\ z_a(k) \cdot \left(\hat{m}^{k+2} - 2(\hat{m}-1)^{k+2} + (\hat{m}-2)^{k+2}\right), & \hat{m} \geq 2 \end{cases} \tag{39}$$

where $z_a(k) := a^{-k}(k+1)^{-1} - a^{-k}(k+2)^{-1}$.

One other class of risk measures are the upside and downside risk measures. The upside risk measure is given by

$$\tilde{\rho}(\tilde{\Lambda}_M) = \mathbb{E}[(\tilde{\Lambda}_M - K)^+],$$

and the downside risk is given by

$$\tilde{\rho}(\tilde{\Lambda}_M) = \mathbb{E}[(K - \tilde{\Lambda}_M)^+],$$

where $K \in \mathbb{R}^+$ is some constant. The upside risk measure enables us to gauge the expected gain of $\tilde{\Lambda}_M$ beyond some threshold value K, whereas downside risk enables us to measure the loss in $\tilde{\Lambda}_M$ below some threshold value K. Such upside and downside risk measures are popular in industry because many firms are interested in determining their expected performance, relative to some benchmark or constant K. Additionally, unlike other risk measures these risk measures take into account behavioral finance concepts in measuring risk, such as Prospect Theory. Such behavioral theories imply that individuals actually gauge risk relative to some benchmark or "reference point" K, hence these risk measures are more realistic in measuring risk. Moreover, such upside and downside risk measures are coherent (Szegö, 2005) hence they will measure risk correctly.

To estimate the upside risk for parameter $K \geq 0$, define the shifted grid by $y_n = KT + (n-1)\Delta$, $n = 1, \ldots, N/2$, and recover the terminal density $f_{Y_M}(y)$ using $y_1 = KT$.[1] We can then calculate

$$\mathbb{E}[(\tilde{\Lambda}_M - K)^+] = T^{-1} \cdot \mathbb{E}[(Y_M - KT)^+] \approx \Upsilon_{a,N}^{[1]} \sum_{1 \leq n \leq N/2} \bar{\beta}_{a,n}^{[1]} \varrho_n(K), \tag{40}$$

where the coefficients are defined by

$$\varrho_n(K) = T^{-1} a^{-1} \cdot \begin{cases} 1/6, & n = 1 \\ n - 1, & n \geq 2. \end{cases} \tag{41}$$

6 Numerical Experiments

In this section we calculate political risk using a number of risk measures. We consider the Heston stochastic volatility model, as described earlier in the paper, because this is one of the most popular stochastic volatility models but also takes into account a wide range of volatility dynamics. Whilst the specifications of the model are not important to the method, we include them here for completeness

$$\begin{aligned} dX(t)/X(t) &= r dt + \sigma(t) dB^1(t), \\ d\sigma^2(t) &= \mu_2(\tilde{\kappa} - \sigma^2(t)) dt + \tilde{\eta} \sigma(t) dB^2(t), \end{aligned}$$

where $corr(dB^1(t), dB^2(t)) = \rho = -0.7, \tilde{\eta} = 0.15, \mu_2 = 1, r = 0, \tilde{\kappa} = 0.02, \sigma_0 = 0.04$. Whilst it is possible to calibrate the Heston model to real world market data, which would provide risk measurement results related to real market data, we restrict our analysis to the specified model values. The reader is referred to papers such as (Cui et al., 2017a), or (Escobar and Gschnaidtner, 2016), for more information on calibrating the Heston model to real world market data.

[1] Before we had used $y_1 = 0$.

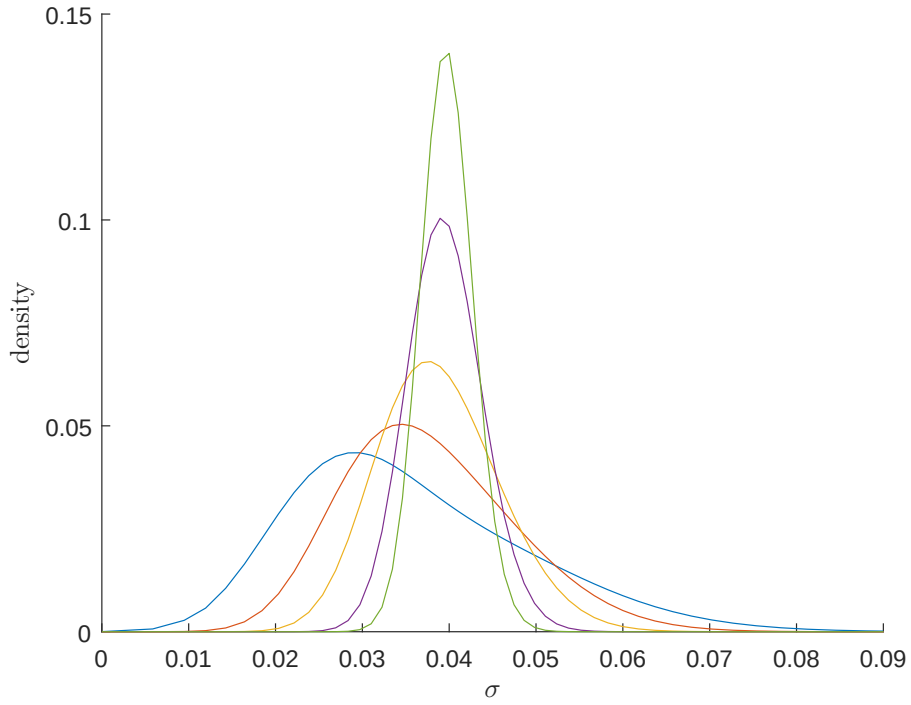

Figure 1: CTMC conditional density of volatility process under Heston stochastic volatility

In Figure 1, we illustrate the conditional transition densities of the volatility process for a model with $n = 40$ Markov states. Hence we model 40 political states, and so this provides a wide range of political climates. We also vary the time step between $\Delta t \in \{1/100, 1/50, 1/20, 1/10, 1/5\}$, where densities are progressively decreasing in peakedness for Δ_t, starting from $\Delta t = 1/100$. As can be seen in the figure, from the initial state $\sigma_0 = 0.04$ the densities shift leftward towards the long run level $\bar{\kappa} = 0.02$ as Δt increases. When $\Delta t = 1/100$, the transition density is tightly centered around the σ_0, while as Δt increases, the probability mass is spread more evenly across the possible states. In this particular example, the starting state is one for which there is greater political uncertainty, compared to the longer term level of $\bar{\kappa}$, and over time, the volatility has a tendency to revert to $\bar{\kappa}$. In this sense, $\bar{\kappa}$ allows us to capture the mode of "long term" political conditions.

In Figure 2 we plot the transition densities of the terminal realized variance ($T = 1$), conditioned on the starting state σ_0, as σ_0 varies along a nonuniform grid over [1e-05, 0.1406] with $n = 40$ grid points. The leftmost peaked density corresponds to the initial variance level $\sigma(0) = 0.0039$, and the rightmost density corresponds to $\sigma(0) = 0.1357$, with the remaining densities starting from values of $\sigma(0)$ between these two boundaries.

Even with a modest number of volatility states, we obtain a relatively smooth distribution for the realized variance, over $[0, T]$. As one can see from the figure, when the initial volatility state nears zero, the integrated variance becomes tightly concentrated, as the volatility is starting in a more "dormant" or low risk state. As the initial risk level increases, the distribution spreads

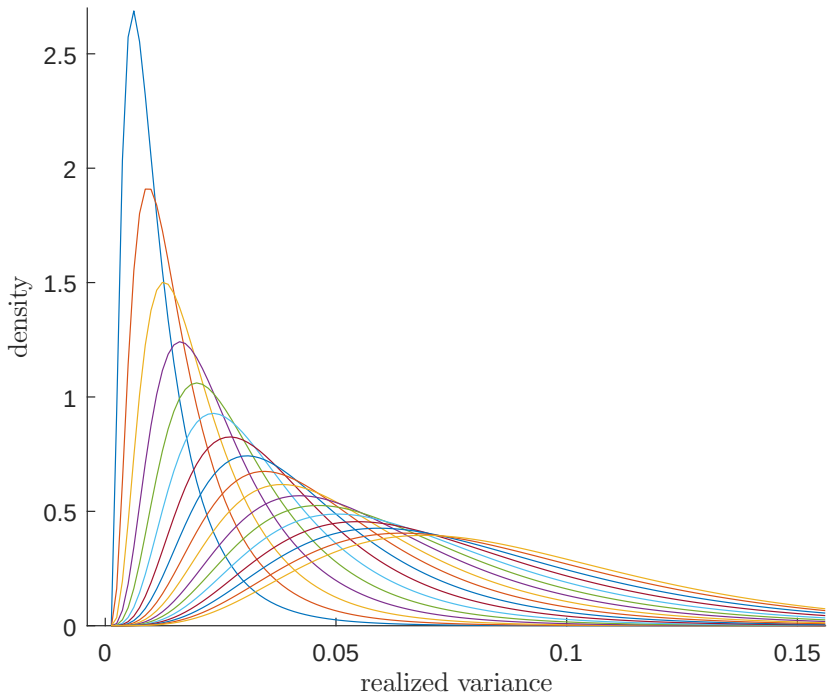

Figure 2: Realized variance conditional density of CTMC derived from Heston stochastic volatility

its mass more evenly and symmetrically around the starting volatility.

One appealing aspect of the proposed framework is that as the number of political states increases, the model of political risk converges in distribution to a well understood stochastic volatility model. In Figure 3 we illustrate the convergence of the expected value of realized variance under the CTMC model to the Heston model which is used to generate the latent states. The model "error" err is defined as

$$err = \mathbb{E}[\Lambda_M^n] - \mathbb{E}[\Lambda_M^*],$$

where $\mathbb{E}[\Lambda_M^n]$ is the expected realized variance calculated from the n-state CTMC model using the PROJ method, and $\mathbb{E}[\Lambda_M^*]$ is the exact expected value under Heston's model. The exact values are calculated for the Heston model using the closed-form solution given in (Bernard and Cui, 2014). As can be observed by the figure, the model error decreases as the number of states n increases. Hence these results reflect that the finite state political risk model converges to the volatility process underlying Heston's model, namely the CIR process.

To test for robustness in our model we determine the deviation in expected realized variance values from the true values in Heston's model, in Tables 3 and 4, . In both tables we test different observation parameters $M \in \{5, 12, 54, 180, 360\}$, we also test for $T = 1$ and $T = 0.5$ in Table 3 and Table 4, respectively. The true values are obtained using the analytical values computed by the method of (Bernard and Cui, 2014), and are denoted by the column "BC", the PROJ method is used to calculate CTMC values for an $n = 40$ state model. The tables serve to

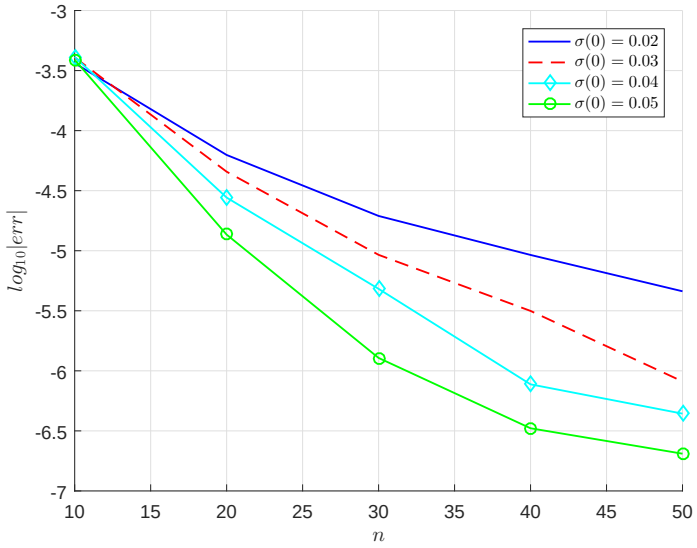

Figure 3: Convergence of expected value of realized variance under political risk model derived from Heston stochastic volatility.

illustrate the closeness of the model to the theoretical stochastic volatility model. To provide a baseline for the "errors" observed we also provide Monte Carlo (MC) simulation with 10^5 simulations, we use Euler's method with a sub-stepping approach of 40 steps per discretization interval of length $\Delta_t = T/M$.Additionally we also apply a control variate to reduce variance, using the analytically available expected value in this case.

The errors are calculated against the baseline BC method, and are denoted as

$$E_{PROJ} := |PROJ - BC|, \text{ and } E_{MC} := |MC - BC|.$$

	$\rho = -0.7$						$\rho = 0$					
M	BC	PROJ	MC	E_{PROJ}	E_{MC}	Std.Err	BC	PROJ	MC	E_{PROJ}	E_{MC}	Std.Err
5	0.033031	0.033073	0.032839	4.16e-05	1.89e-05	8.00e-05	0.032706	0.032705	0.032557	1.10e-06	1.49e-04	8.00e-05
12	0.032809	0.032851	0.032727	4.20e-05	5.22e-05	5.52e-05	0.032669	0.032669	0.032598	9.72e-08	7.14e-05	5.88e-05
54	0.032680	0.032721	0.032656	4.15e-05	3.30e-05	3.58e-05	0.032648	0.032648	0.032656	8.63e-08	7.70e-06	4.27e-05
180	0.032654	0.032695	0.032658	4.15e-05	2.40e-05	3.08e-05	0.032644	0.032644	0.032673	6.65e-08	2.92e-05	3.85e-05
360	0.032648	0.032690	0.032653	4.16e-05	2.15e-05	2.94e-05	0.032643	0.032643	0.032668	1.15e-07	2.51e-05	3.75e-05

Table 3: Expected value of realized variance ($T = 1$) for an $n = 40$ state model, derived from Heston.

	$\rho = -0.7$						$\rho = 0$					
M	BC	PROJ	MC	E_{PROJ}	E_{MC}	Std.Err	BC	PROJ	MC	E_{PROJ}	E_{MC}	Std.Err
5	0.035957	0.035961	0.035796	3.97e-06	1.61e-04	8.24e-05	0.035774	0.035772	0.035668	2.54e-06	1.07e-04	8.14e-05
12	0.035831	0.035837	0.035724	6.39e-06	1.07e-04	5.62e-05	0.035754	0.035754	0.035705	6.59e-07	4.91e-05	5.79e-05
54	0.035759	0.035764	0.035713	4.95e-06	4.67e-05	3.54e-05	0.035742	0.035741	0.035754	6.66e-07	1.22e-05	3.90e-05
180	0.035745	0.035751	0.035799	5.70e-06	5.43e-05	2.94e-05	0.035740	0.035740	0.035735	1.24e-07	5.04e-06	3.39e-05
360	0.035742	0.035748	0.035724	5.86e-06	1.82e-05	2.79e-05	0.035739	0.035739	0.035709	2.79e-08	3.04e-05	3.27e-05

Table 4: Expected value of realized variance ($T = 0.5$) for an $n = 40$ state model, derived from Heston.

We now wish to calculate risk using the risk measures discussed in Section 5. One common risk measure is *upside risk*, which is

$$\mathbb{E}[(\Lambda_M - K)^+], \quad K \geq 0. \tag{42}$$

In Table 5 we calculate upside risk (defined by equation (42)) for several values of the parameter $K \in \{0.01, 0.02, ..., 0.05\}$ along each column in the table, with $T = 1$ for convenience. We do this for two sets of correlation values $\rho = -0.7$ and $\rho = 0$. Additionally, we vary the number of monitoring dates $M \in \{5, ..., 360\}$ for each row of the table, and M defines the realized variance in Λ_M.

	$\rho = -0.7$					$\rho = 0$				
M / K	0.01	0.02	0.03	0.04	0.05	0.01	0.02	0.03	0.04	0.05
5	0.023488	0.015973	0.010817	0.007416	0.005170	0.023188	0.015712	0.010457	0.006920	0.004580
12	0.022926	0.014330	0.008452	0.004907	0.002856	0.022784	0.014243	0.008254	0.004585	0.002494
54	0.022727	0.013323	0.006559	0.002875	0.001181	0.022665	0.013318	0.006504	0.002755	0.001062
180	0.022698	0.013141	0.006087	0.002344	0.000794	0.022653	0.013141	0.006072	0.002296	0.000746
360	0.022692	0.013104	0.005980	0.002220	0.000708	0.022651	0.013104	0.005975	0.002191	0.000677

Table 5: Upside Risk Measurement Under Heston Stochastic Volatility Model With $n = 40$ Latent States

As can be seen by Table 5, a change in correlation from negative correlation ($\rho = -0.7$) to independence ($\rho = 0$) leads to noticeably different results. The negative correlation $\rho = -0.7$ reflects the leverage effect that exists in many assets, whilst $\rho = 0$ implies independence between volatility and asset price. A negative correlation results in higher political risk (measured in terms of upside risk) for all equivalent input parameters, compared to zero correlation. This is a satisfying result because leverage (negative correlation) is typically associated with higher risk. We can also see from the table the convergence of realized variance, Λ_M, as M increases. However, comparing $M = 5$ to $M = 360$, we can see that number of observations points can also significantly impact the estimated risk.

We calculate moment based risk measures in the following two tables. The tables demonstrate the ability of the proposed framework to faithfully estimate moment-based risk measures of the political risk model. We consider kth moments of realized variance, $\mathbb{E}[\Lambda_M^k]$, for $k \in \{1, 2, 3, 4\}$, and compare the estimates to Monte Carlo. Table 6 and Table 7 provide estimates for $T = 1$ and $T = 0.5$, respectively. As the value of k increases, the moments $\mathbb{E}[\Lambda_M^k]$ quickly diminish, although there is close agreement between PROJ and Monte Carlo at all levels, with the differences mostly falling within two standard deviations.

	$\rho = -0.7$				$\rho = 0$			
k	PROJ	MC	Std.Err	Diff	PROJ	MC	Std.Err	Diff
1	0.032851	0.032688	6.20e-05	1.63e-04	0.032669	0.032630	5.89e-05	3.96e-05
2	0.001466	0.001461	6.84e-06	4.92e-06	0.001416	0.001413	5.84e-06	3.40e-06
3	0.000088	0.000087	9.12e-07	3.02e-07	0.000079	0.000078	6.29e-07	6.10e-07
4	0.000007	0.000007	2.51e-07	1.03e-07	0.000005	0.000005	7.51e-08	8.30e-08

Table 6: Moments (k) of realized variance ($T = 1$), $M = 12$, for an $n = 40$ state model.

	$\rho = -0.7$				$\rho = 0$			
k	PROJ	MC	Std.Err	Diff	PROJ	MC	Std.Err	Diff
1	0.035837	0.035867	6.00e-05	2.99e-05	0.035754	0.035638	5.80e-05	1.15e-04
2	0.001647	0.001645	6.52e-06	2.63e-06	0.001615	0.001609	5.80e-06	5.92e-06
3	0.000096	0.000095	7.41e-07	1.41e-06	0.000090	0.000089	5.66e-07	9.75e-07
4	0.000007	0.000007	1.09e-07	1.58e-07	0.000006	0.000006	7.45e-08	6.20e-08

Table 7: Moments (k) of realized variance ($T = 0.5$), $M = 12$, for an $n = 40$ state model.

	$\rho = -0.7$				$\rho = 0$			
p	PROJ	MC	Std.Err	Diff	PROJ	MC	Std.Err	Diff
0.50	0.028222	0.028173	6.62e-05	4.93e-05	0.028811	0.028734	6.94e-05	7.68e-05
0.75	0.041197	0.041134	1.08e-04	6.29e-05	0.041706	0.041674	2.89e-05	3.17e-05
0.90	0.057739	0.057726	1.58e-04	1.26e-05	0.057011	0.056937	1.88e-04	7.38e-05
0.95	0.070465	0.070352	1.67e-04	1.13e-04	0.068201	0.068016	3.91e-04	1.84e-04
0.99	0.101492	0.101042	6.54e-04	4.50e-04	0.094159	0.093508	6.05e-04	6.51e-04

Table 8: VaR of realized variance ($T = 1$), $M = 12$, for an $n = 40$ state model.

The final set of experiments illustrate the calculation of Value-at-Risk (VaR) in Tables 8 and 9. One observation to notice is that as the VaR level increases, the standard error of the Monte Carlo estimation also increase as the difficulty in estimation of rare events (by simulation) also increases.

	$\rho = -0.7$				$\rho = 0$			
p	PROJ	MC	Std.Err	Diff	PROJ	MC	Std.Err	Diff
0.50	0.031839	0.031779	8.09e-05	5.97e-05	0.032314	0.032252	4.94e-05	6.22e-05
0.75	0.044665	0.044580	7.85e-05	8.49e-05	0.045143	0.045123	1.22e-04	2.01e-05
0.90	0.060283	0.060173	1.57e-04	1.10e-04	0.059895	0.059770	9.85e-05	1.25e-04
0.95	0.071972	0.071911	1.12e-04	6.17e-05	0.070438	0.070276	1.12e-04	1.62e-04
0.99	0.099785	0.099014	6.29e-04	7.71e-04	0.094315	0.093928	5.28e-04	3.88e-04

Table 9: VaR of realized variance ($T = 0.5$), $M = 12$, for an $n = 40$ state model.

The ability to measure political risk is useful for risk management purposes. It enables us to identify, evaluate and prioritise the political risk with respect to different assets and investments. As a result of political risk measurement, one can determine whether it is more beneficial to avoid political risk for some investments, or implement strategies to reduce or share some political risks (for instance purchasing some political risk insurance products). Alternatively, if political risk is unavoidable, political risk measurement can enable one determine the level of financial reserves required to budget for such risks.

7 Conclusion

Political risk modelling has gained increasing attention in research literature, and has direct implications for social risks such as civil disorder. Consequently, the modelling of political risks are important to social as well as economic reasons. In this paper we have proposed a model for political risk, which can be applied to mathematical finance models. To the best of our knowledge this is the first model for continuous time stochastic volatility models. Hence this paper will be of interest to academics and industry.

We derive a number of important properties in our political risk model, in particular, we derive a solution for the characteristic function and we prove weak convergence. Both of these properties are important to ensuring our model is related to the authentic volatility process of the asset pricing model, and correctly modelling risk. We derive a method for calculating standard risk measures for our political risk, namely Value at Risk, variance, moments, as well as upside and downside risk measurements. We also provide numerical experiments to illustrate our results.

In terms of future work, we would like to investigate contagion risk modelling from political risk, for instance the cross market linkages of political risk in one country have been empirically shown to impact the political risk in neighbouring and allied countries. The continuous time processes of political risk transmission have yet to be investigated. Secondly, we would like to examine the systemic and idiosyncratic components of political risk for different countries, particularly with respect to developed and emerging markets. This would potentially lead

to enabling the formulation of diversified political risk portfolios. Finally, we would like to investigate the impact of political risk on different asset classes and derivatives. For example, it is known that some asset classes are affected by particular risk factors more than other asset classes. Consequently, we need to model the asset classes that have higher exposure to political risk compared to other asset classes.

References

Artzner, P., F. Delbaen, J. Eber, D. Heath, and H. Ku (2003). Coherent multiperiod risk measurement. *Manuscript, ETH Zurich* .

Beazer, Q. H. and D. J. Blake (2018). The conditional nature of political risk: How home institutions influence the location of foreign direct investment. *American Journal of Political Science* 62(2), 470485.

Beckers, S. (1980). The Constant Elasticity of Variance Model and Its Implications For Option Pricing. *The Journal of Finance* 35(3), 661–673.

Bekaert, G., C. R. Harvey, C. T. Lundblad, and S. Siegel (2016). Political risk and international valuation. *Journal of Corporate Finance* 37, 123.

Bernard, C. and Z. Cui (2014). Prices and asymptotics for discrete variance swaps. *Applied Mathematical Finance* 21(2), 140–173.

Bittlingmayer, G. (1998). Output, stock volatility, and political uncertainty in a natural experiment: Germany, 1880-1940. *The Journal of Finance* 53(6), 22432257.

Black, F. and M. Scholes (1973). The pricing of options and corporate liabilities. *Journal of Political Economy* 81(3), 637654.

Bodie, Z., A. Kane, and A. J. Marcus (2019). *Essentials of investments.* McGraw-Hill Education.

Buffington, J. and R. Elliott (2002). American options with regime switching. *International Journal of Theoretical and Applied Finance* 5(5), 497–514.

Chen, H., H. Liao, B.-J. Tang, and Y.-M. Wei (2016). Impacts of opecs political risk on the international crude oil prices: An empirical analysis based on the svar models. *Energy Economics* 57, 4249.

Clark, E. (2017). *Evaluating Country Risks For International Investments: Tools, Techniques and Applications.* World Scientific Publishing Company.

Cox, J., J. Ingersoll Jr, and S. Ross (1985). A Theory of the Term Structure of Interest Rates. *Econometrica* 53(2), 385–407.

Cox, J. and S. Ross (1976). The Valuation of Options for Alternative Stochastic Processes. *Journal of Financial Economics* 3(1), 145–66.

Cui, Y., S. D. B. Rollin, and G. Germano (2017a). Full and fast calibration of the heston stochastic volatility model. *European Journal of Operational Research* 263(2), 625638.

Cui, Z., J. L. Kirkby, and D. Nguyen (2017b). A general framework for discretely sampled realized variance derivatives in stochastic volatility models with jumps. *European Journal of Operational Research* 262(1), 381400.

Dimic, N., V. Orlov, and V. Piljak (2015). The political risk factor in emerging, frontier, and developed stock markets. *Finance Research Letters* 15, 239245.

Dupire, B. (1994). Pricing with a smile. *Risk* 7(1), 18–20.

Escobar, M. and C. Gschnaidtner (2016). Parameters recovery via calibration in the heston model: A comprehensive review. *Wilmott* 2016(86), 6081.

Fang, F. and C. W. Oosterlee (2009). A novel pricing method for european options based on fourier-cosine series expansions. *SIAM Journal on Scientific Computing* 31(2), 826848.

Filippou, I., A. E. Gozluklu, and M. P. Taylor (2018). Global political risk and currency momentum. *Journal of Financial and Quantitative Analysis* 53(05), 22272259.

Heston, S. (1993). A Closed-Form Solution for Options with Stochastic Volatility with Applications to Bond and Currency Options. *Review of Financial Studies* 6(2), 327–43.

Hull, J. and A. White (1987). The Pricing of Options on Assets with Stochastic Volatilities. *The Journal of Finance* 42(2), 281–300.

Johnson, H. and D. Shanno (1987). Option Pricing when the Variance is Changing. *The Journal of Financial and Quantitative Analysis* 22(2), 143–151.

Kelly, B., L. Pastor, and P. Veronesi (2016). The price of political uncertainty: Theory and evidence from the option market. *The Journal of Finance* 71(5), 24172480.

Kirkby, J. (2015). Efficient option pricing by frame duality with the fast Fourier transform. *SIAM J. Financial Mathematics* 6(1), 713–747.

Kirkby, J., D. Nguyen, and Z. Cui (2017). A unified approach to Bermudan and barrier options under stochastic volatility models with jumps. *J. Economic Dynamics and Control* 80, 75–100.

Kirkby, J. L. (2017). Robust option pricing with characteristic functions and the b-spline order of density projection. *Journal of Computational Finance, (forthcoming)* .

Lo, C. C. and K. Skindilias (2014). An improved markov chain approximation methodology: Derivatives pricing and model calibration. *International Journal of Theoretical and Applied Finance* 17(07), 1450047.

Lu, S.-L. (2009). Comparing the reliability of a discrete-time and a continuous-time markov chain model in determining credit risk. *Applied Economics Letters* 16(11), 11431148.

Markowitz, H. (1952). Portfolio Selection. *The Journal of Finance* 7(1), 77–91.

Merton, R. (1973). Theory of rational option pricing. *Bell Journal of Economics and Management Science* 4(1), 141–183.

Mijatovic, A. and M. Pistorius (2011). Continuously monitored barrier options under markov processes. *Mathematical Finance* 23(1), 138.

Musiela, M. and M. Rutkowski (2005). *Martingale Methods In Financial Modelling*. Springer, New York.

Nordén, L. (2003). Asymmetric option price distribution and bid–ask quotes: consequences for implied volatility smiles. *Journal of Multinational Financial Management* 13(4-5), 423–441.

Pantzalis, C., D. A. Stangeland, and H. J. Turtle (2000). Political elections and the resolution of uncertainty: The international evidence. *Journal of Banking & Finance* 24(10), 15751604.

Schroder, M. (1989). Computing the constant elasticity of variance option pricing formula. *Journal of Finance* 44(1), 211–219.

Scott, L. (1987). Option Pricing when the Variance Changes Randomly: Theory, Estimation, and an Application. *The Journal of Financial and Quantitative Analysis* 22(4), 419–438.

Snowberg, E., J. Wolfers, and E. Zitzewitz (2007). Partisan impacts on the economy: Evidence from prediction markets and close elections. *The Quarterly Journal of Economics* 122(2), 807829.

Szegö, G. (2005). Measures of risk. *European Journal of Operational Research* 163(1), 5–19.

Wilmott, P. et al. (1998). *Derivatives: the theory and practice of financial engineering*. John Wiley & Sons.